UCRL-11001
c.2

University of California

Ernest O. Lawrence Radiation Laboratory

TWO-WEEK LOAN COPY

This is a Library Circulating Copy which may be borrowed for two weeks. For a personal retention copy, call Tech. Info. Division, Ext. 5545

KINETICS AND MECHANISM OF THE ANATASE-RUTILE TRANSFORMATION

Berkeley, California

UCRL-11001
c.2

DISCLAIMER

This document was prepared as an account of work sponsored by the United States Government. While this document is believed to contain correct information, neither the United States Government nor any agency thereof, nor the Regents of the University of California, nor any of their employees, makes any warranty, express or implied, or assumes any legal responsibility for the accuracy, completeness, or usefulness of any information, apparatus, product, or process disclosed, or represents that its use would not infringe privately owned rights. Reference herein to any specific commercial product, process, or service by its trade name, trademark, manufacturer, or otherwise, does not necessarily constitute or imply its endorsement, recommendation, or favoring by the United States Government or any agency thereof, or the Regents of the University of California. The views and opinions of authors expressed herein do not necessarily state or reflect those of the United States Government or any agency thereof or the Regents of the University of California.

UCRL-11001

UNIVERSITY OF CALIFORNIA
Lawrence Radiation Laboratory
Berkeley, California

AEC Contract No. W-7405-eng-48

KINETICS AND MECHANISM OF THE ANATASE-RUTILE TRANSFORMATION

Robert Day Shannon

(Ph. D. Thesis)

March 20, 1964

Printed in USA. Price $2.25. Available from the
Office of Technical Services
U. S. Department of Commerce
Washington 25, D.C.

KINETICS AND MECHANISM OF THE ANATASE-RUTILE TRANSFORMATION

Contents

Abstract v

General Introduction 1

I. Transformation of Single Crystals of Anatase

A. Introduction 3

B. Experimental Procedure and Results 6

C. Mechanism of Transformation 15

D. Discussion 24

II. Nucleation and Growth of Rutile in Single Crystals of Anatase

A. Introduction 25

B. Experimental 25

C. Results and Discussion

1. Nucleation and Growth 26

2. The Origin of Rutile Needles in Anatase Crystals 38

3. Application of Nucleation and Growth Data to the Kinetics of Powder Reactions 39

III. Kinetics of the Powder Reaction

A. Introduction 40

B. Experimental Procedure

1. Experimental Materials 41

2. Procedure 44

C. Results 45

IV. Impurity Effects

A. Introduction 56

B. Experimental Procedure

1. Hydrogen Atmosphere and Vacuum 59

2. Addition of CuO 60

C. Results and Discussion 62

1. The Transformation in Hydrogen- and Vacuum-reducing Atmosphere 62

2. Effects of CuO on the Transformation 67

3. General Considerations of Impurity Effects . . . 74

General Summary 82

Acknowledgments 84

Appendices

A. Rate Laws for Some Solid-State Transformations . . 85

B. Calculation of Equilibrium Vacancy Concentration in Rutile 88

References 89

KINETICS AND MECHANISM OF THE ANATASE-RUTILE TRANSFORMATION

Robert Day Shannon

Lawrence Radiation Laboratory
University of California
Berkeley, California

March 20, 1964

ABSTRACT

We have studied the anatase-rutile transformation using both single crystals and powders. Rutile crystallites that formed when anatase single crystals were heated at 900° to 950°C were found to exhibit preferred orientation. A study of the orientation (Sec. I) led to a mechanism similar to that of the brookite-rutile transformation. The mechanism involves retention of the {112} pseudo-close-packed planes in anatase and rearrangement of the titanium and oxygen ions within the plane. A cooperative movement of the titanium and oxygen ions is proposed in which the majority of the titanium ions, in order to reach their new sites, break two of their original six Ti-O bonds.

Nucleation and growth in anatase thin sections were followed under a hot-stage microscope. Both occurred preferentially at edges, corners, and inclusions (Sec. II). Growth spread two-dimensionally over the surface in some crystals, and propagated three-dimensionally from point sources in others.

Transformation of three commercial anatase powders resulted in sigmoid transformation curves, which were interpreted in terms of a nucleation-growth process (Sec. III). Analysis of these curves by means of several rate laws led to activation energies for nucleation of 110, 135, and 150 kcal/mole, and for growth of 100,

115, and 190 kcal/mole for the three materials.

A literature review made of the effects of impurities on the transformation (Sec. IV) suggested that the rate of transformation is governed by the defect structure of the TiO_2, i.e., by the concentration of oxygen vacancies or titanium interstitials. In this study both CuO additions and a hydrogen atmosphere were found to accelerate the transformation. It is proposed that (a) CuO accelerates the transformation by formation of a substitutional solid solution and a consequent increase in oxygen-vacancy concentration, and (b) hydrogen accelerates the transformation either by the introduction of oxygen vacancies or by reduction to a second Ti_nO_{2n-1} Magnéli phase. A vacuum of 3×10^{-4}-mm Hg was found to retard the rate of transformation. This was attributed to the introduction of titanium interstitials.

GENERAL INTRODUCTION

Titanium dioxide exists in three principal crystalline forms--anatase, brookite, and rutile. Anatase and rutile are of commercial importance, being used extensively as pigment and dielectric materials. Brookite has not been synthesized artificially and is found only as natural single crystals. Brookite and anatase are both metastable forms and transform exothermally to rutile over a range of temperatures, but usually at ≈750° and ≈ 1000°C, respectively.

The anatase structure is metastable at normal transformation temperatures since the transformation at these temperatures is irreversible. The free energy of transformation must be negative, at least above 400°C, since the reaction has been made to proceed at that temperature in the presence of an alkali flux.[1] It is not known whether an equilibrium transformation temperature exists, however, since neither the heat of formation of anatase nor solubility data for the two crystalline forms is known.

Barblan et al.[2] studied the crystallography and mechanism of the brookite-rutile transformation, while Rao et al.[3] determined the kinetics of transformation of brookite powder. An oriented transformation was found which allowed Barblan et al.[2] to postulate a mechanism involving (a) shifting of some of the Ti atoms to new sites and (b) a general rearrangement of the oxygen ions. The kinetic study showed a reaction controlled in the initial stages by nucleation and in the latter stages by growth. The overall activation energy[3] was 65 kcal/mole.

The anatase-rutile transition is of greater interest to the ceramist than the brookite transition because of the use of anatase as a pigment and as a raw material in ceramic systems. The methods of synthesis of anatase and rutile have generally been (a) high-temperature oxidation of titanium halides, and (b) hydrolysis of sulfate solutions. The environment in which formation of the TiO_2 takes

place greatly affects both the resulting crystalline form and the anatase-rutile transition temperature when anatase is the chief product. An extensive literature survey revealed that much work has been done to determine how the method of preparation and the presence of additives affect the stability of anatase. The effective transformation temperature varies from 400° to 1200°C, depending on the presence of certain impurities. The presence of the sulfate or phosphate ion results in high transformation temperatures while alkali or halide ions tend to reduce the transformation temperature. The most effective accelerator[4] was found to be CuO when added to the crystalline TiO_2, while the most effective inhibitor was shown to be the phosphate ion when added during the crystallization process.[5] The effect of a vacuum-reducing atmosphere was found by Czanderna et al.[6] to be insignificant, although Iida and Ozaki[4] found that the transformation was accelerated in vacuum and hydrogen atmospheres.

The kinetics of transformation of synthetic anatase were determined by Cole and Sullivan[7] and Rao.[8] As in the transformation of brookite, the process was found to be a nucleation-growth phenomenon. The activation energy per mole varied from 80 kcal for pure TiO_2 to 110 kcal for relatively impure commercial TiO_2.

Although much data exists on methods of preparation, on the effects of additives, and on the kinetics of transformation, no general understanding of the transformation has yet evolved. In order to ascertain more basic information about the mechanism of the transformation and the factors which control the rate of transformation, we made a detailed crystallographic and kinetic study. Section I shows the results of a preferred orientation study obtained when anatase single crystals are transformed. An explicit mechanism is derived from rutile pole figures. In Section II, the observation under a hot-stage microscope of the nucleation and growth of rutile from anatase single crystals is described. Section III is concerned with the kinetics of transformation of several commercial brands of titania powders. Finally, the effects of CuO and heating in hydrogen- and vacuum-reducing atmospheres are described in Sec. IV.

I. TRANSFORMATION OF SINGLE CRYSTALS

A. Introduction

It is frequently possible to determine the mechanism of crystallographic phase transformations by studying the orientation of the product phase with respect to that of the reactant. If the transformation occurs so that the orientation of the product phase is correlated with the orientation of the reactant phase, then a topotactical relation is said to exist.* [9-13] The degree of correlation determines the degree of topotaxy. If the atoms undergo only a change in secondary coordination and no primary bonds are broken, such as in displacive phase transformations, then a high degree of topotaxy results. A crystal undergoing such a reaction results in a single-crystal diffraction pattern before and after the transformation. If, however, the atoms must undergo extensive rearrangement, little accord exists between the original and final structures and the transformation is weakly topotactical or reconstructive. The dehydroxylation of γ-FeOOH to form γ-Fe_2O_3,[12] and the α-β quartz transformation are two examples of strong topotaxy. Cases of intermediate and weak topotaxy occur, respectively, in the dehydration of $Mg(OH)_2$ and $Ca(OH)_2$,[14] while the quartz-cristobalite transformation is reconstructive,[15] and is thus not expected to exhibit tototaxy.

---

*Bernal (1960)[11] and Mackay[12] (1960) use more restricted criteria of (a) the retention of at least one axis of symmetry, or (b) a three-dimensional accord between the structures and preservation of the majority of the atomic positions. Taylor et al.[13] (1962) assume Lotgering's definition, with the added restriction that three-dimensional accord between the initial and final structures is present.

A study of the brookite-rutile transformation[2] revealed a moderately topotactical transformation and allowed the investigators to postulate a mechanism involving small atomic rearrangements. The brookite [100] was found to remain coincident with the rutile [100]. In the brookite (100) plane, the rutile assumed three different orientations: (a) at 700°C, rutile [001] || brookite [001]; (b) at 800°C, rutile [001] || brookite [010]; and (c) at 800°C, rutile [001] || brookite [027] or [023]. In a [100] projection of the brookite structure, zig-zag chains of TiO_6 octahedra running along the c-axis are evident so that formation of the chains of octahedra in rutile in case (a) is not unexpected and involves only a straightening of the chains and a breaking up of every other octahedron by a shift of the Ti atom from its original octahedral site to a new site. In cases (b) and (c) the movement required of the oxygen atoms is less than that in case (a), but the movement of the Ti atoms is greater. Barblan et al.[2] suggested that the mobility of the oxygen atoms relative to that of the Ti atoms is greater at lower temperatures, making case (a) reasonable. As the temperature increases, the mobility of the Ti atoms becomes greater and case (b) becomes predominant. The same authors made an attempt to find similar behavior in the anatase-rutile transformation but failed to discover any preferred orientation of the rutile crystals. From Table I it can be seen that the volume change in the brookite-rutile transition is $\approx 3\%$, while that in the anatase-rutile transition is $\approx 8\%$; thus, in the latter case, a more random distribution of the rutile crystals can be expected from the distortion alone.

Our experiments have shown, however, that large octahedral single crystals of anatase could be transformed without loss of their external shape even though severe cracks had developed. The fact that the crystals were still bipyramidal in shape and had not disintegrated allowed us to determine the orientation of the product phase by x-ray diffraction methods. We hoped that a study of this orientation would provide some information concerning movements of the atoms during the transformation.

Table I. Properties of TiO_2.

Form	Symmetry	Space group	Unit cell dimensions (Å)	Calculated density (gm/cm^3)
Brookite	Orthorhombic	D_{2h}^{15} Pbca	a = 9.18[a] b = 5.45 c = 5.14	4.126
Anatase	Tetragonal	D_{4h}^{19} $I\frac{4}{a}md$	a = 3.785[b] c = 9.514	3.892
Rutile	Tetragonal	D_{4h}^{14} $P\frac{4}{m}nm$	a = 4.593[c] c = 2.959	4.249

[a]Pauling, L., and Sturdivant, J. H., Zeits. Krist. 68, 239-56 (1928).

[b,c]Cromer, D. T., and Herrington, K., J. Am. Chem. Soc. 77 [18], 4708-09 (1955).

B. Experimental Procedure and Results

Three crystals were chosen for a detailed orientation study. The first crystal, G-2,* from Disentis, Graubünden, Switzerland, was a bipyramid 0.5 mm × 0.2 mm, the long dimension being along the c-axis. The other two crystals, V-2 and V-4,** from the area of Val Vals, Graubünden, Switzerland, were large bipyramidal crystals, one 4 mm × 2 mm, and the other, 1.5 mm × 1 mm. Crystal G-2 was heated at 850°C for 28 h, 900° for 66 h, 926° for 25 h, and at 950° for 10 h. Crystal V-2 was heated for 3 h at 850°, 3 h at 900° and 1 h at 950°C. Crystal V-4 was heated for 48 h at 900°, after which it developed severe cracks throughout (Fig. 1). The transformation was found to proceed from the surface of the crystal toward the center. This behavior, combined with the large shrinkage, necessitated the formation of these cracks. Crystal G-2 was transparent and tan in color before the transformation, and brilliant orange afterward; the other two crystals, being less pure, were translucent and dark green in color.

Rotation patterns resulted in discontinuous rutile powder rings, indicating polycrystalline specimens exhibiting preferred orientation. Determination of the orientation of the rutile crystallites was made in a manner similar to that used in the study of preferred orientation in metal wires and sheets.[16] When a polycrystalline specimen exhibiting preferred orientation is irradiated with monochromatic x-rays, discontinuous powder rings result. If the crystallite size is large, oscillation patterns, rather than stationary patterns, must be used. Oscillation patterns provide the angle ρ which the normals to the reflecting planes make with the axis of oscillation. The intersection of the cone of angle 2ρ with the cone of angle $180° - 2\theta$, whose axis is the incident x-ray beam, gives the position of the pole. These poles can then be plotted on a stereogram. A series of oscillation

---

*Obtained from Minerals Unlimited, Berkeley, California.

**Obtained from Scott Williams Mineral Co., Inc., Scottsdale, Arizona.

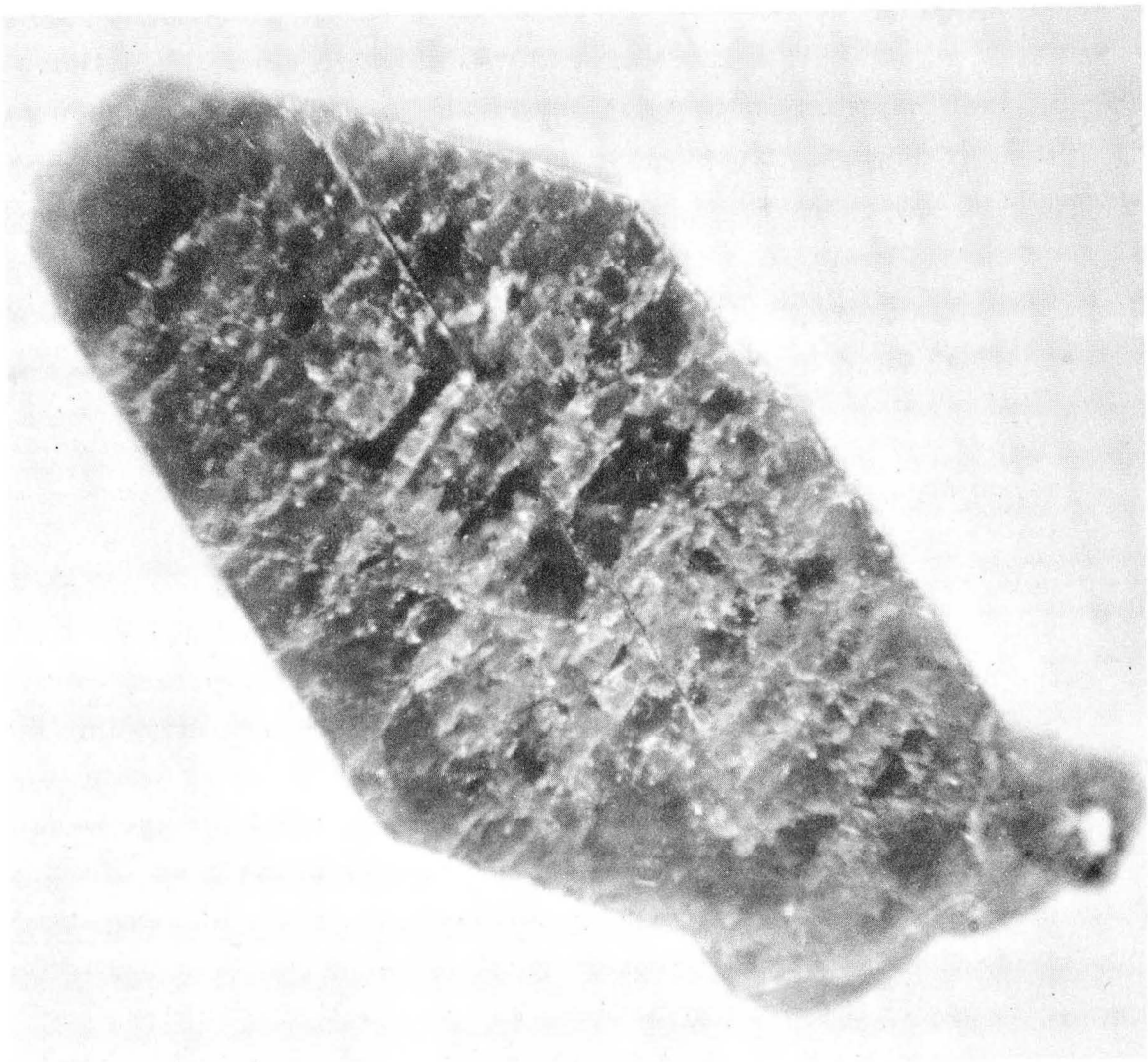

ZN-4151

Fig. 1. Section through crystal V-4 ⊥ [100].

patterns made with the incident x-ray beam oriented in different positions with respect to the original anatase crystals provide the complete pole figure.

Each heat-treated crystal was mounted in an oscillation camera so that the c-axis of the original anatase crystal was perpendicular to the x-ray beam. Ten-degree oscillation patterns using filtered Cu radiation were made at appropriate intervals around the [001] axis for crystals V-2 and V-4, and around the [001] and [100] axes for crystal G-2. The rutile (110) rather than the (100) poles were chosen because of their relatively high intensity. A typical pattern showing rutile preferred orientation in crystal G-2 is seen in Fig 2b , which may be compared to the pattern shown in Fig. 2a for a sample of randomly oriented rutile powder. The diffraction rings were analyzed for crystals V-2, V-4, and G-2 to provide the rutile (110) and (001) pole figures shown in Figs. 3a, 3b, and 3c. Composite diagrams for both the [001] and [100] orientations of the original anatase, in which the pole figures for the three crystals were superimposed, were also constructed. Figures 4a and 4b show the composite diagrams for the anatase [100] and [001] orientations.

The regions of intensity within the diffraction rings were sometimes discontinuous because of the large size of the crystallites. The large degree of scatter in the positions of the poles was evidently caused by the distortion resulting from the shrinkage and cracking accompanying the transformation. Despite these difficulties, regions of concentration of the rutile (110) and (001) poles are evident in the pole figures. It can be seen that clustering of the (110) poles occurs around the equator and around the anatase [001], and that the (001) poles are situated at a latitude of about 45 deg.

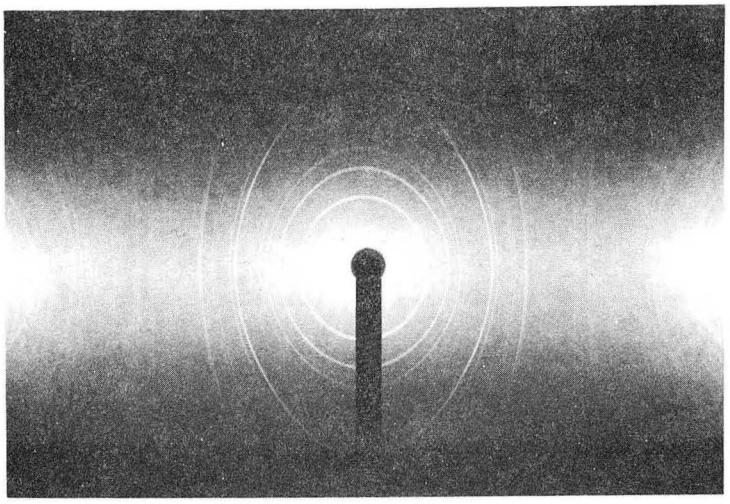

(a)

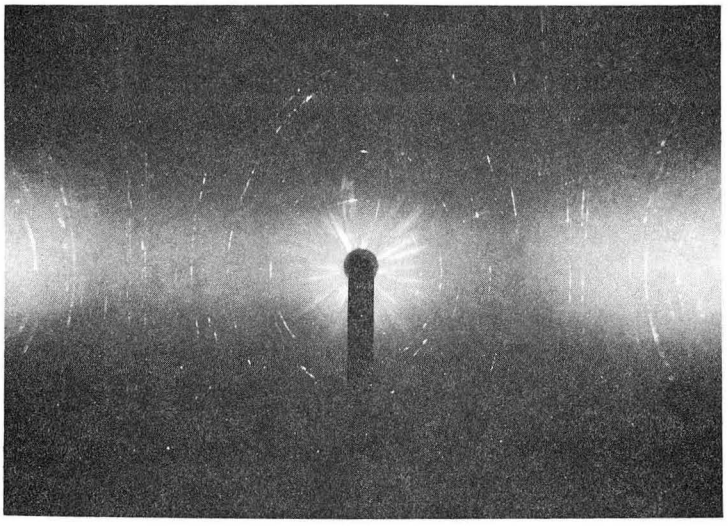

(b)

ZN-4263

Fig. 2. (a) Random powder pattern of rutile.
(b) Ten-degree oscillation pattern of crystal G-2 showing discontinuous rutile diffraction rings.

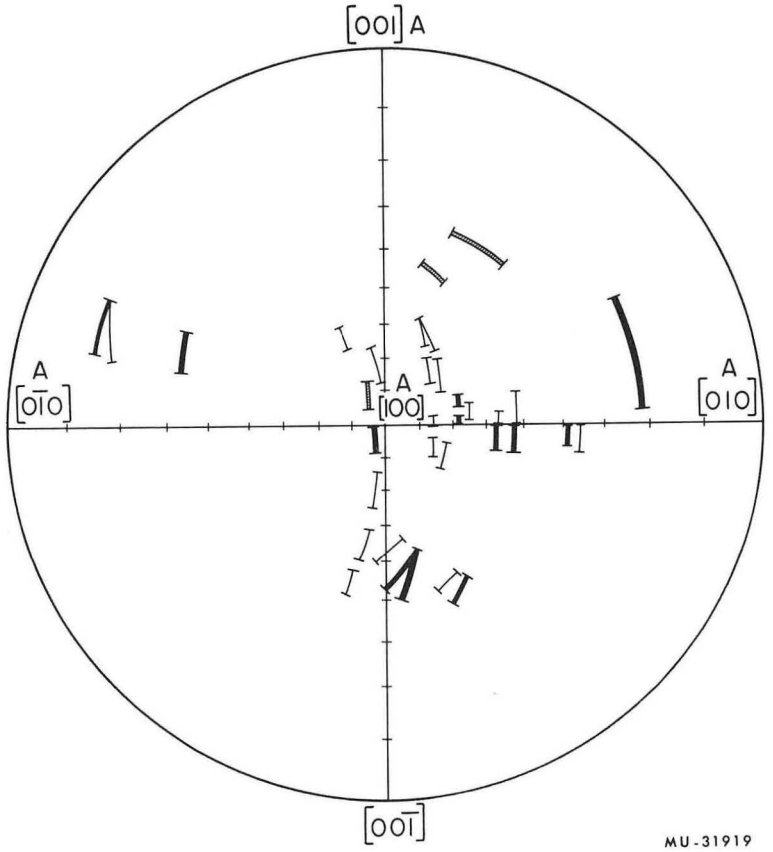

Fig. 3. (a) Pole figure showing rutile (110) and (001) poles superimposed on a [100] anatase projection, crystal V-2.

(110) pole, high intensity reflection

(110) pole, low intensity reflection

(001) pole, high intensity reflection

(001) pole, low intensity reflection

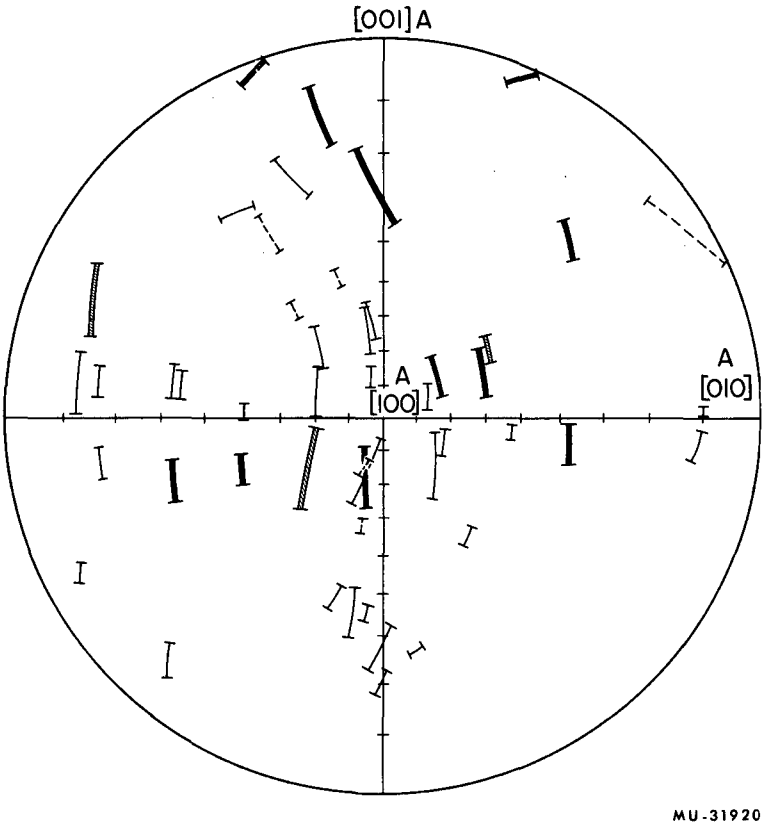

Fig. 3. (b) Crystal V-4; see caption for Fig. 3(a).

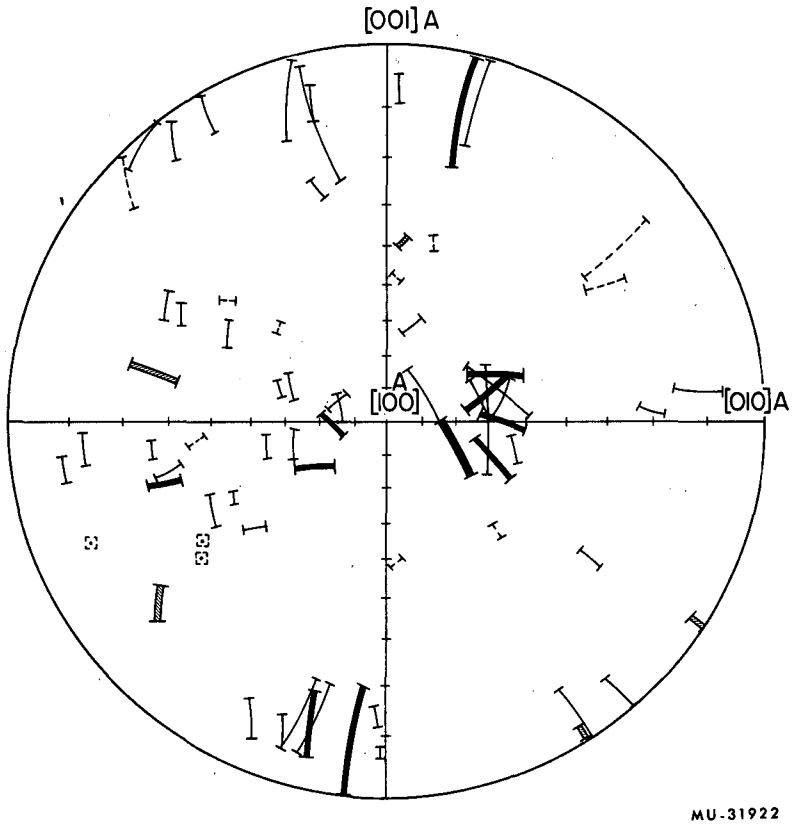

Fig. 3. (b) Crystal G-2; see caption for Fig. 3(a).

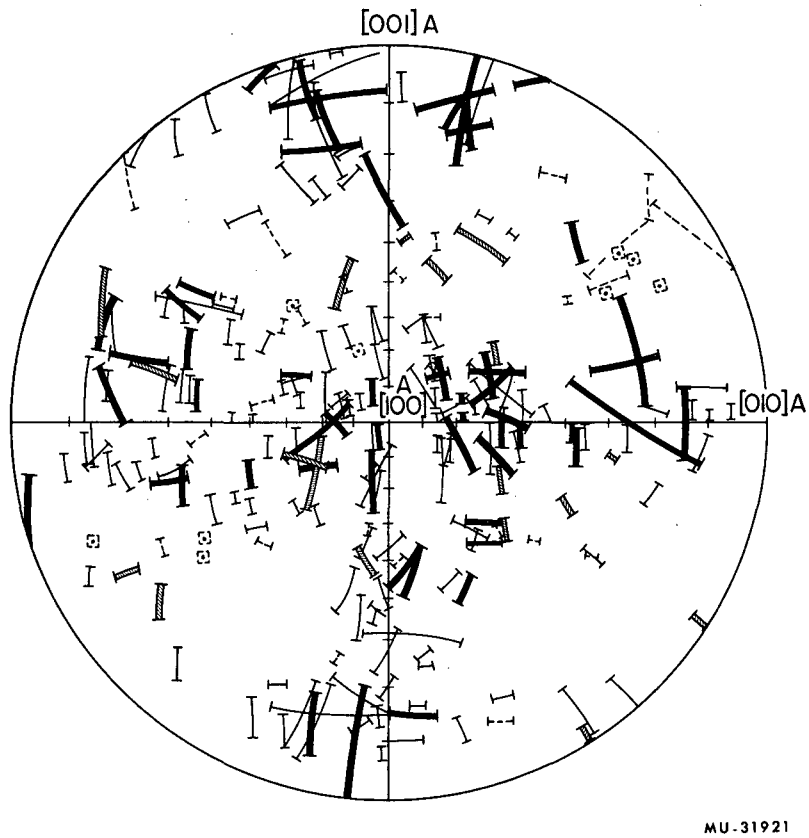

Fig. 4. (a) Composite pole figure showing rutile (110) and (001) poles on a [100] projection of crystals V-2, V-4, and G-2.

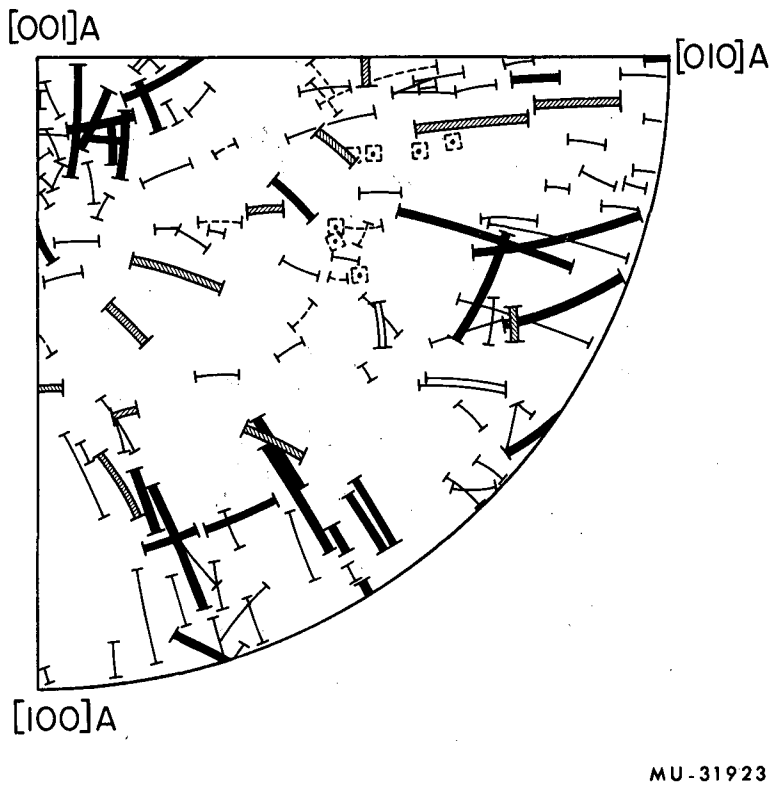

Fig. 4. (b) Composite pole figure showing rutile (110) and (001) poles on a [001] projection of crystals V-2, V-4, and G-2.

C. Mechanism of Transformation

From a study of the kinetics of the reaction (Sec. III), it is apparent that the mechanism cannot be a mere change of bond angles and/or bond lengths which result in a slight shift or retention of major crystallographic axes. The activation energy was found to vary among different samples (depending upon the impurity content) from 100 to 180 kcal/mole. These values suggest that the process involves the rupture of bonds and a major rearrangement of atoms. In addition, an examination of the anatase and rutile structures did not reveal any close similarity, thus indicating the necessity of a rearrangement of atoms.

The anatase and rutile structures can be represented as sodium chloride structures with half the cations removed and the anions slightly offset from their normal positions.[17] Then it is possible to consider the two structures to be made up of pseudo-close-packed oxygen layers with different arrangements of the Ti atoms (see Figs. 5a, 5b, and 5c). In anatase the close-packed plane is the (112) plane with the Ti atoms arranged in zig-zag chains running along [221] as indicated in Fig. 5a. For the sake of clarity, only one oxygen plane with its associated titanium ions is shown. Actually, four of these planes are necessary to cover the repeat distance. In the next layer of oxygen atoms, the zig-zag chains of titanium ions are displaced along [110] by half the distance between chains and along [221] by 0.6Å. Figure 5b shows part of the second oxygen layer. In rutile the close-packed plane is (100) and the Ti atoms lie in rows along [001] as indicated in Fig. 5c. The rutile structure may also be pictured as a series of chains of TiO_6 octahedra parallel to the c-axis, where each octahedron shares two of its opposite edges with two other octahedra. The Ti atoms in the [001] rows form the centers of these octahedra, some of which are shown in Fig. 5c.

The anion framework is expected to remain intact if the least spatial disturbance of the structure is to take place. Since the interplanar spacings of the close-packed planes in anatase and rutile are

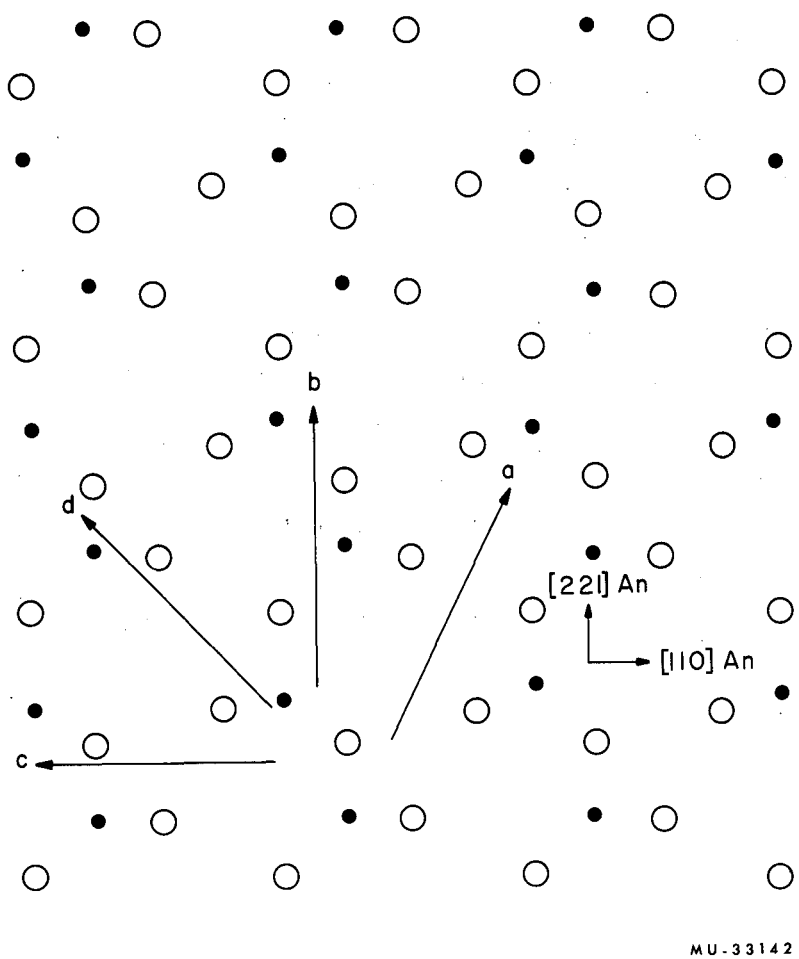

Fig. 5. (a) Projection perpendicular to the (112) pseudo-close-packed plane in anatase showing possible directions of the rutile c-axes.

○ oxygen ions

● titanium ions

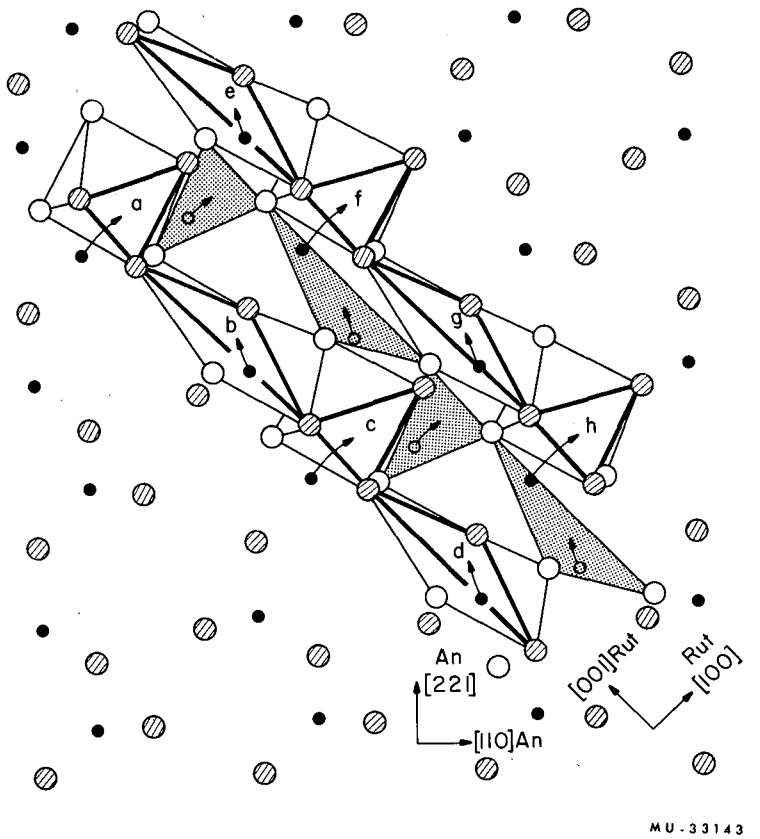

Fig. 5 (b) The (112) plane in anatase showing the rutile octahedral structure.

- ⊘ oxygen ions in the upper plane
- ● titanium ions below the upper plane of oxygen ions
- ○ oxygen ions in the lower plane
- o titanium ions below the lower plane of oxygen ions

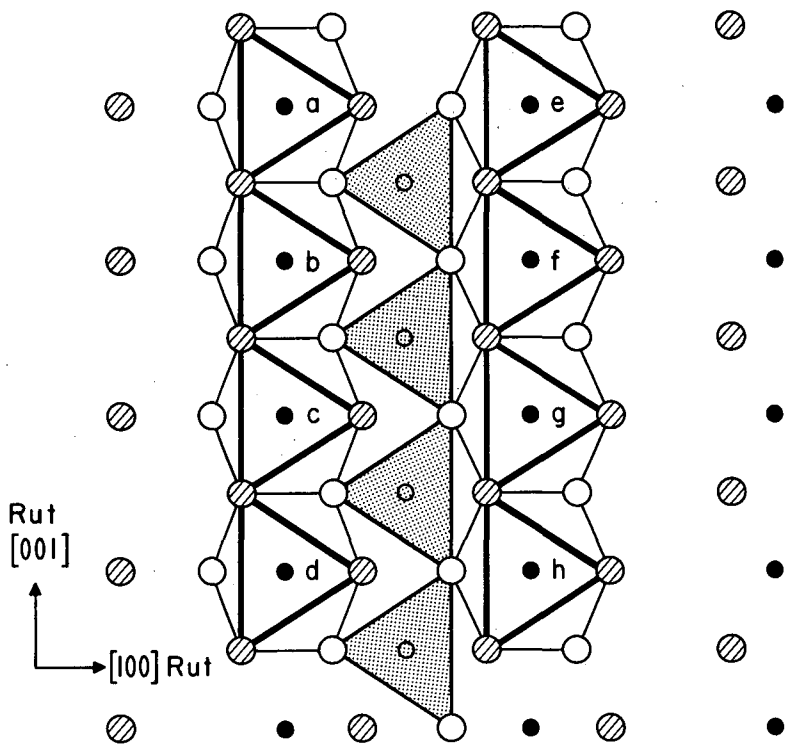

MU-33975

Fig. 5. (c) Projection perpendicular to the (100) pseudo-close-packed plane in rutile showing the rutile octahedral structure.

nearly identical (d^{anat}_{112} = 2.336; d^{rut}_{200} = 2.297), it was assumed that most of the atomic movement occurred within the planes themselves. Since the Ti atoms lie in rows in the rutile structure, one looks for similar rows in the anatase (112) plane. The possible directions for the resultant rutile c-axis are indicated in Fig. 5a. Directions "a", "b", and "c" do not result in the experimentally observed distribution of (110) and (001) planes. The line of atoms along "d" is clearly the direction in which most of the [001] poles were found. Figure 6a is a stereogram showing the trace of one of the (112) planes containing two directions which the c-axes of rutile may assume after the transformation. Figure 6b shows the orientation of four of the eight possible equivalent rutile unit cells and the complete pole figure which would be anticipated if the resultant rutile crystals grew in all possible orientations. Although the positions of the calculated poles (Fig. 6b) do not lie exactly at the center of the experimental intensity distribution (Fig. 4a), the agreement is considered satisfactory in light of the large amount of shrinkage and distortion which takes place during the transformation.

The mechanism of the transformation appears to be similar to that of brookite in the sense that the close-packed planes in the reactant remain as close-packed planes in the product with almost the same spacing while the major rearrangement occurs within these planes. Figure 4b shows the atoms of the rutile TiO_6 octahedral structure as they are arranged in anatase before the transformation. In achieving the rutile configuration shown in Fig. 5c, considerable distortion occurs, as may be seen from the relative positions of the atoms shown in the figures. In the lower layer, half the titanium atoms undergo no change in nearest neighbors, while the other half break two Ti-O bonds and acquire two new nearest neighbors. In the upper layer all the cations must break two bonds in achieving their new position. It is clear from the positions of the cations in Figs. 5b and 5c that a shrinkage of approximately 20% occurs in the new [001] direction and an expansion of approximately 10% occurs in the new [100] direction.

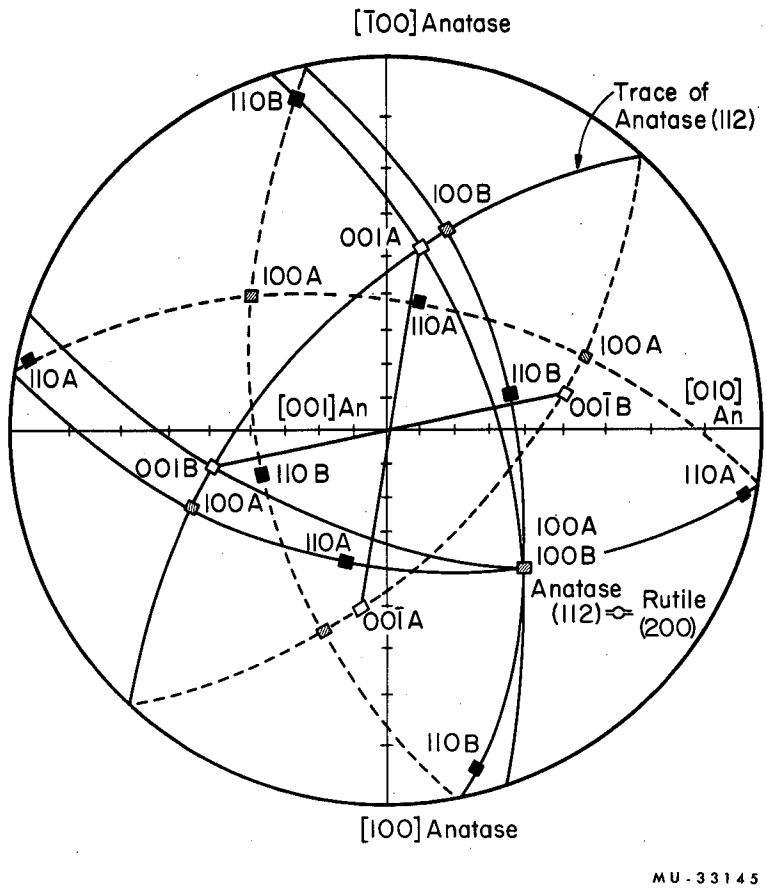

Fig. 6. (a) An anatase [100] stereogram showing the orientation of two rutile crystals whose c-axes lie in an anatase (112) plane.

▨ rutile (110)

□ rutile (001)

▨ rutile (100)

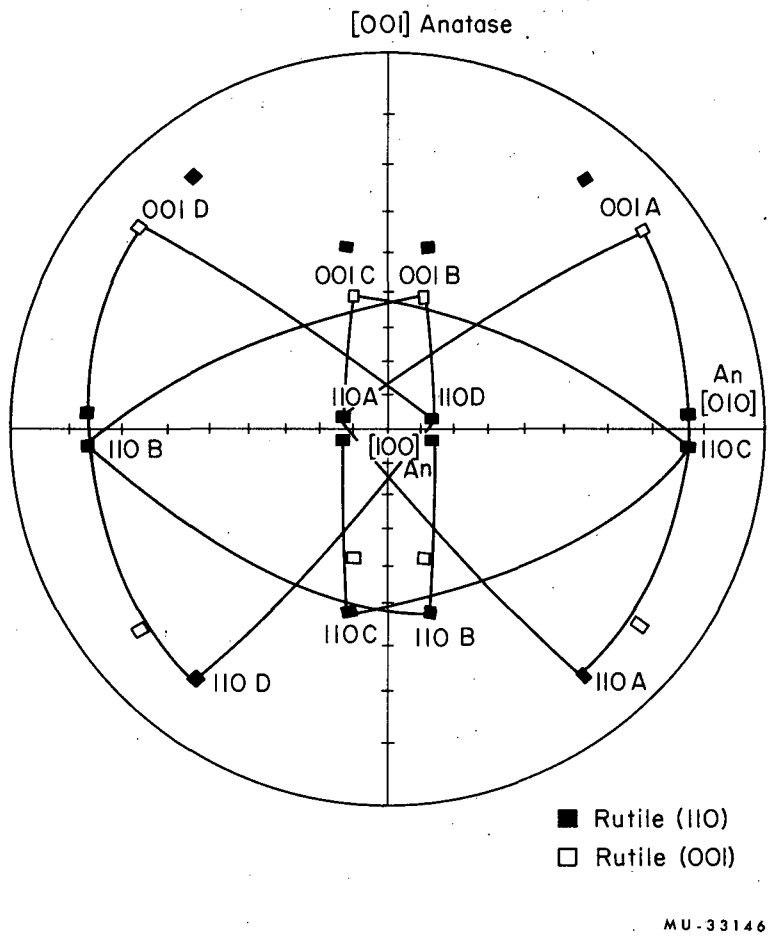

Fig. 6. (b) Anatase [100] stereogram showing rutile (110) and (001) poles and the orientation of four equivalent rutile crystals.

Figure 7 shows two adjacent cations and the surrounding oxygen configuration (a) before, and (b) after the transformation. Figure 7a corresponds to Fig. 5b and shows octahedra a and b in anatase, while Fig. 7b shows the rutile octahedra a and b indicated in Fig. 5c. The dimensional changes noted above allow a closing of the oxygen configuration on the right and a relaxation of the configuration on the left, allowing the shifts of the titanium atoms to their new octahedral sites between 3 "a" atoms and 3 "b" atoms as a consequence of the anion movement. These shifts occur by the cation breaking two bonds indicated by dashed lines in the diagram and result in the cations having four nearest neighbors and two more distant neighbors at the midpoint of the movement. The apparent movement of the cations into tetrahedral sites does not actually occur because what were previously tetrahedral sites have become octahedral sites as a consequence of the indicated oxygen movements and the associated rearrangement. This mechanism is best described as a cooperative movement of the titanium and oxygen ions and is in contrast to a diffusion mechanism in which the anion structure remains essentially fixed.

The question then remains why the rutile c-axes fail to lie in the "a", "b" or "c" directions as indicated in Fig. 5a. From a careful consideration of the movements that would be necessary to align titanium atoms in the "b" direction, we find that a cooperative movement of the atoms similar to that in the "d" direction is required. Rearrangement in this direction, however, would involve greater distortion of the oxygen configuration and would require an expansion along this direction. Consideration of the movements that would be necessary for alignment of the titanium atoms in the "a" or "c" direction show that the distortion of the oxygen atom configuration is not great. However, a diffusion type of movement of half the cations in an anion structure that remains essentially fixed would be necessary. Such a movement would have required that only two original neighbors be retained, thus breaking four Ti-O bonds.

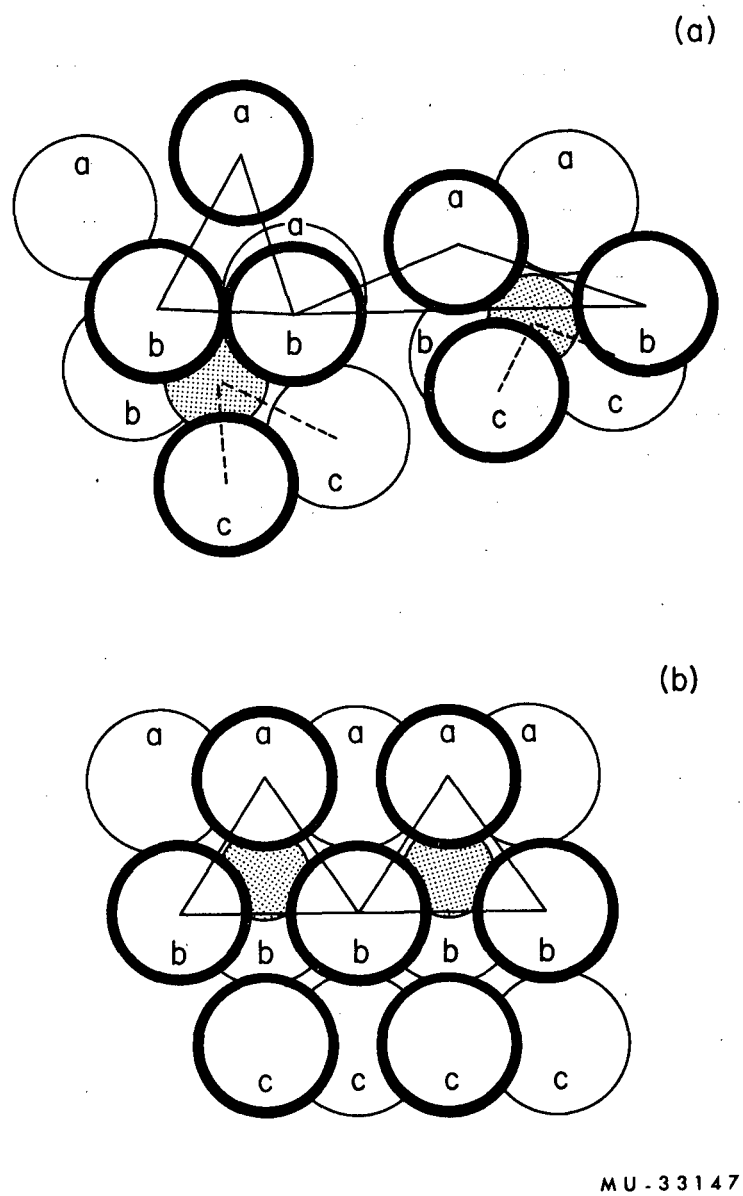

Fig. 7. (a) The configuration of the octahedral structure in anatase before the transformation, showing the same group of atoms indicated in Fig. 5(b), i.e., a projection perpendicular to the anatase (112) plane. The dashed lines represent Ti-O bonds that are broken as a consequence of the movement of the titanium ions. (b) The octahedral structure of rutile, perpendicular to the rutile (100) plane as in Fig. 5(c).

D. Discussion

The assumption that oriented transformations occur with the least spatial disturbance[18] appears correct, since it implies that the minimum degree of movement and rearrangement of atoms results in the path of minimum energy. However, spatial disturbance must refer to changes in position of the largest structure-determining ions, and the change in distribution of the remaining ions. Thus, it appears from the above that the transformation is controlled by two factors: (1) not only must the principle of the least spatial disturbance of oxygen ions be obeyed, but also (2) the number of bonds broken must be a minimum. The activation energy should therefore be made up of two terms: the strain energy which must be overcome for the oxygen atoms in the close-packed planes to reach their new configuration, and the energy necessary to break the Ti-O bonds as the titanium atoms redistribute themselves.

Strong topotaxy implies similarity of the initial and final structures and the preservation of at least one of the axes of symmetry. The anatase-rutile transformation is not expected, therefore, to be highly topotactical because the structures are dissimilar and none of the major axes of symmetry of the product correspond to those of the reactant. However, neither is the transformation reconstructive or heteromorphous (no dimensional accord between reactant and product), because this type of reaction is characterized by random orientation of the product. Since the product exhibits preferred orientation, it could be classified as an intermediate case of topotaxy. Intermediate cases of topotaxy should occur when only some of the structural elements are preserved. Such cases would include the anatase and brookite transformations, and reactions involving substances with layer structures in which the layers are retained with reconstruction within the layers. In the TiO_2 transitions, retention of the anatase (112) and the brookite (100) planes accompanied by considerable rearrangement of both the cation and anion configurations within the planes results in intermediate cases of topotaxy. The higher degree of topotaxy exhibited by brookite is a result of the smaller dimensional change.

II. NUCLEATION AND GROWTH OF RUTILE IN SINGLE CRYSTALS OF ANATASE

A. Introduction

Knowledge of the mode of nucleation and growth in a phase transformation is frequently useful in estimating the relative rates of these processes and in determining the appropriate kinetic expression for the reaction rates of powders. An application of kinetic rate laws to the transformation of anatase powders requires a theoretical model. An interface reaction implies movement of the interface from all points toward the center of the crystal and is generally treated as a reaction involving a shrinking sphere, thus simplifying the geometry. In Sec. I it was indicated that the transformation had progressed from the surface of the crystal toward the interior. This conclusion was reached after obtaining Laue photographs from the surface of the sectioned crystal V-4 indicating that the center of the crystal was untransformed.

The purposes of this study were to determine: (a) whether nucleation occurred at a few discrete points or whether it occurred instantaneously over the entire surface, and (b) whether the reaction, once nucleated, progressed toward the center of the crystal as an interface reaction. In order to accomplish these two objectives, we observed the transformation of natural crystals of anatase under a hot-stage microscope.

B. Experimental

The hot stage of the microscope was a platinum strip heater type used by Scott and Pask[19] and modified to operate in an air atmosphere because TiO_2 is reduced in vacuum at high temperatures. The temperature was measured by a Pt-Pt-10% Rh thermocouple in contact with the strip heater and placed as close to the crystal as possible.

Five of the crystals (series V) (obtained from Minerals Unlimited, Berkeley, Calif.) were from Val Vals, Grisons, Sw. The other crystal (G3)(obtained from Scott Williams, Scottsdale, Ariz.) was found near Disentis, Grisons, Sw. All of the specimens were in

the form of {101} bipyramids. In general, they were impure crystals with numerous inclusions and discolorations and were characterized by the presence of sheaves of rutile needles extending throughout the body of each crystal (Figs. 8a-8d). The needles were identified as rutile from a rotating crystal pattern taken on a bundle of crystals extracted from the matrix. Rutile needles are frequently prismatic with their c-axes parallel to the prism; however, the pattern did not show such a [001] orientation along the length of the bundle. Crystal G3 was the only one free of both inclusions and needles.

Sections of the six crystals were prepared perpendicular to the axes [001], [100], or [101] and polished with Linde "A" alumina powder. The crystals were heated until the desired stage of nucleation or growth had been attained and were then quenched in air. The rutile growth appeared opaque under transmitted light and was thus easily identified. Photographs were taken after each cycle.

C. Results and Discussion

1. Nucleation and Growth

Various types of nucleation sites were observed: inclusions, corners and edges, surface scratches, and linear imperfections in the interior of the crystal. A summary of nucleation and growth data is presented in Table II. Nucleation occurred at scratches in crystals V7, V9, and V10 (Figs. 12b and 13c) at 1000°C, while in sample G3, needles formed in the interior of the crystal.

Corners and edges served as nucleation sites in crystals G3, V7, and V10 at 1050°C with crystal V10 exhibiting particularly rapid nucleation at the tip of the bipyramid. Crystal G3 showed nucleation occurring simultaneously at most of the edges and corners. In crystal V7, inclusions and already existing rutile needles served as nucleation sites (Figs. 12a-12c show different stages of growth in crystal V7); the needle pointing diagonally to the left served as a rapid growth site.

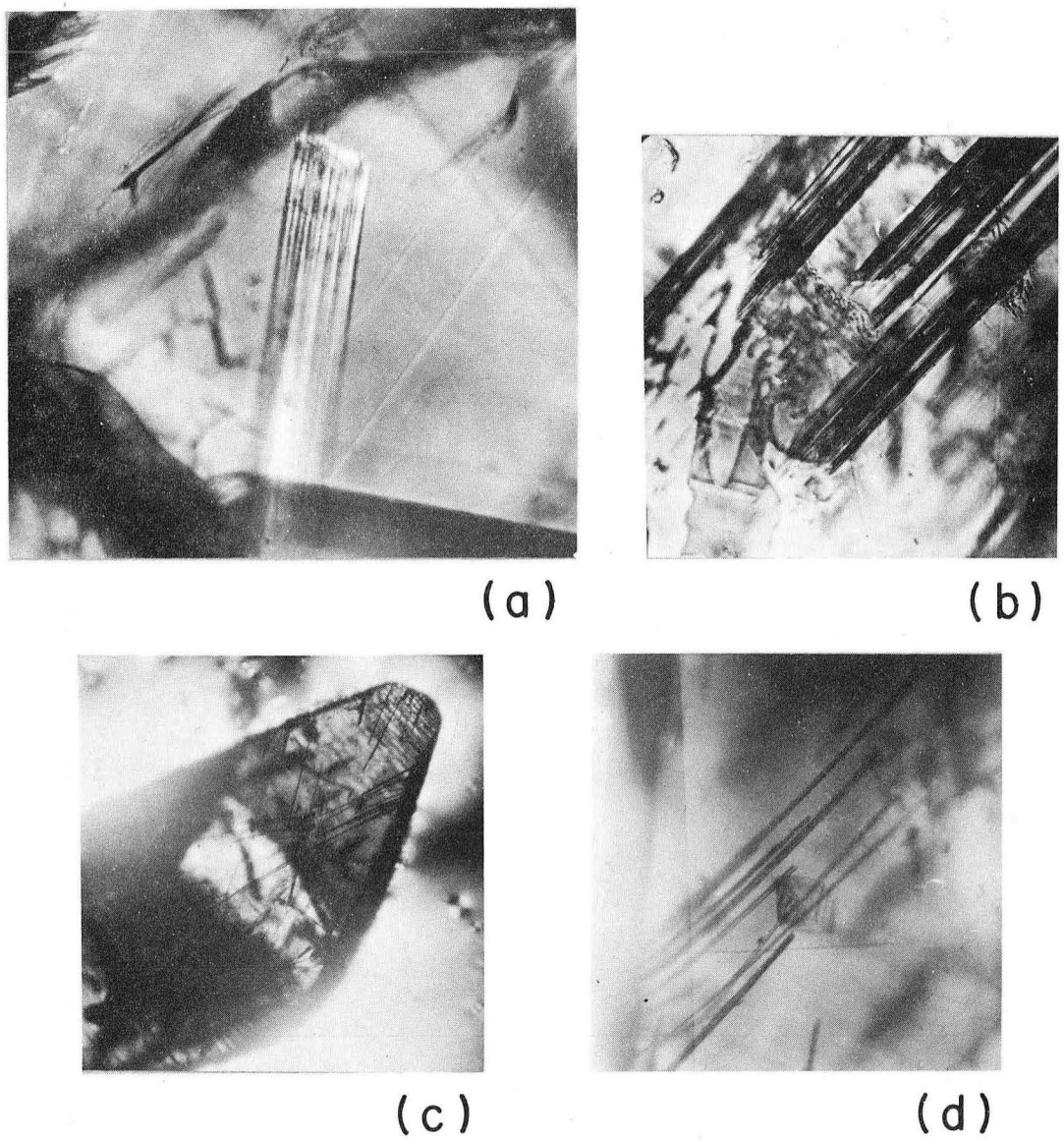

ZN-4264

Fig. 8. Appearance of rutile needles in anatase crystals: (a) Crystal V-1, ×292, crossed Nicols; (b) Crystal V-5, ×292, crossed Nicols; (c) Crystal V-6, ×17, crossed Nicols; (d) Crystal V-6, ×66, crossed Nicols.

Table II. Summary of data for nucleation and growth of rutile in anatase single crystals.

Crystal	Orientation	Nucleation sites	Temp.	Figure No.	Growth sites	Temp.	Figure No.
G3	[101]	Interior channels	1000°C	9a-9c, 10b	Edges and corners	980°C	11a-11e, 10b
		Edges and corners	1050°C				
V7	[100]	Scratches Inclusions Rutile needles	1000°	12a-12h	Inclusions Rutile needles	1060°	12a-12h
V8	[001]	Scratches Inclusions Points on the surface	1050°	13a-13d	Inclusions Points on the surface	1060°	13a-13d
V9	[001]	Scratches	1100°C		Intersection of scratches		
V10	[100]	Scratches Edge Rutile needle			Scratches and intersections of scratches Edge Rutile needle		
V10a	[100]	Corner (tip of bipyramid)			Corner		

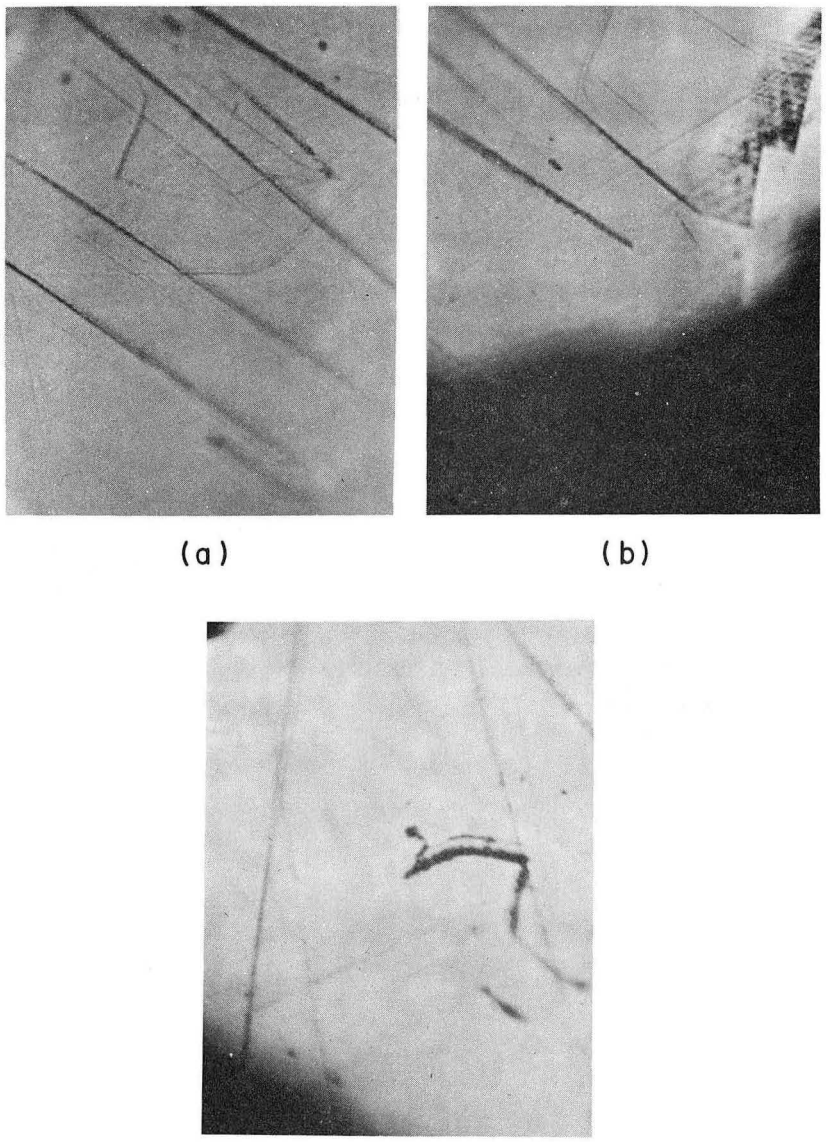

ZN-4265

Fig. 9. Appearance of needles in crystal G-3, ×440, crossed Nicols.

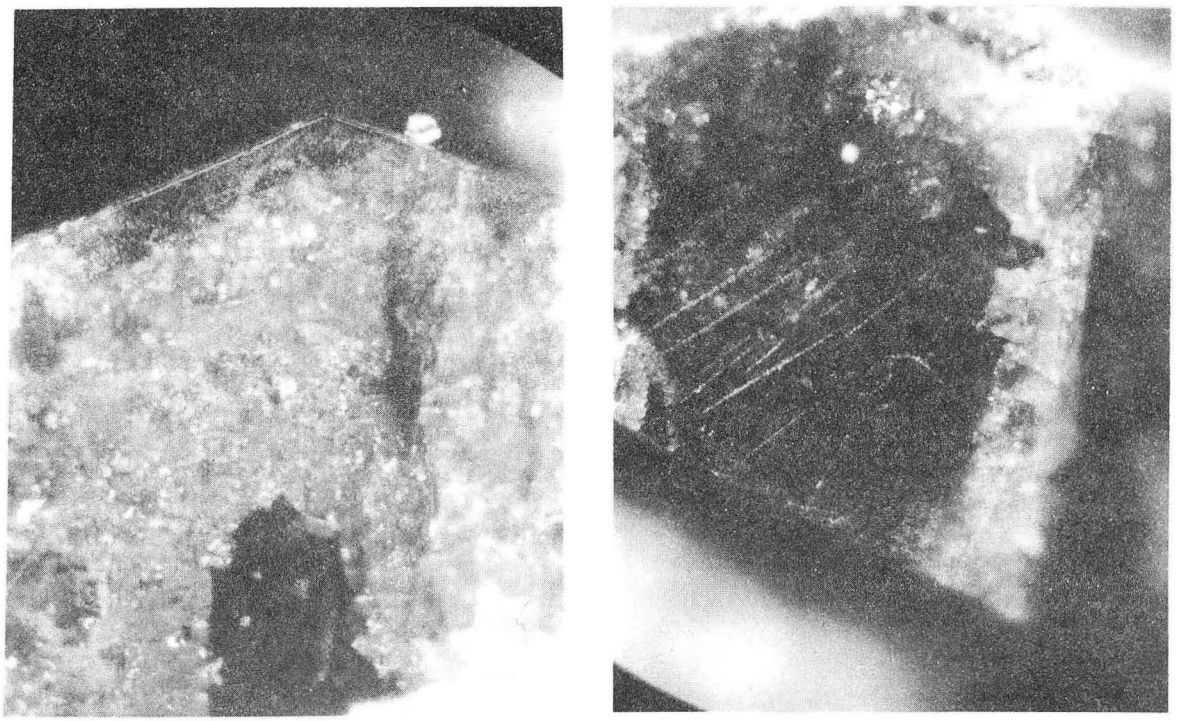

(a) (b)

ZN-4266

Fig. 10. (a) Rutile growth on top surface of crystal G-3, ×110, reflected light; (b) bottom surface of crystal G-3, showing needle growth, ×110, reflected light.

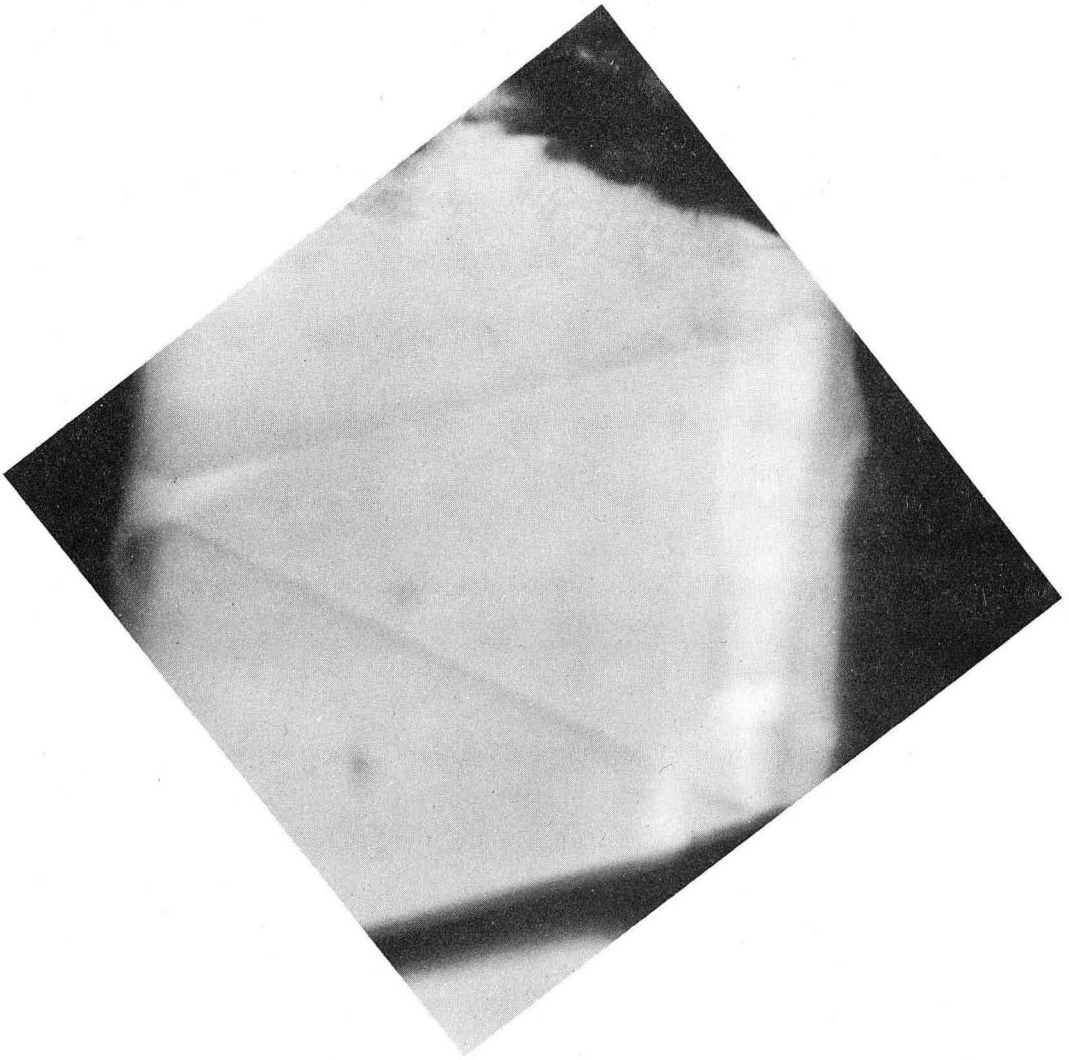

(a)

ZN-4258

Fig. 11. (a) Crystal G-3 before transformation, ×66, crossed Nicols.

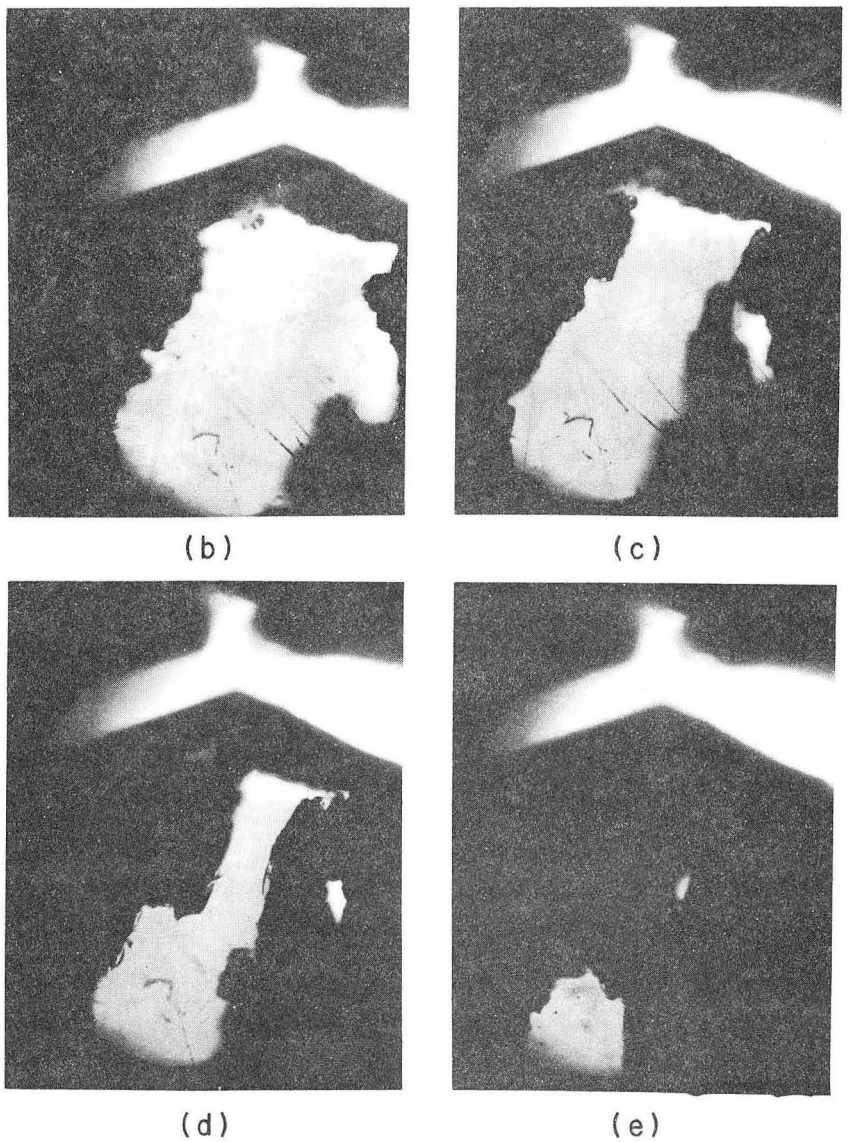

ZN-4267

Fig. 11. (b-e) Photomicrographs showing steps in growth of rutile on the top surface of crystal G-3, ×110, crossed Nicols.

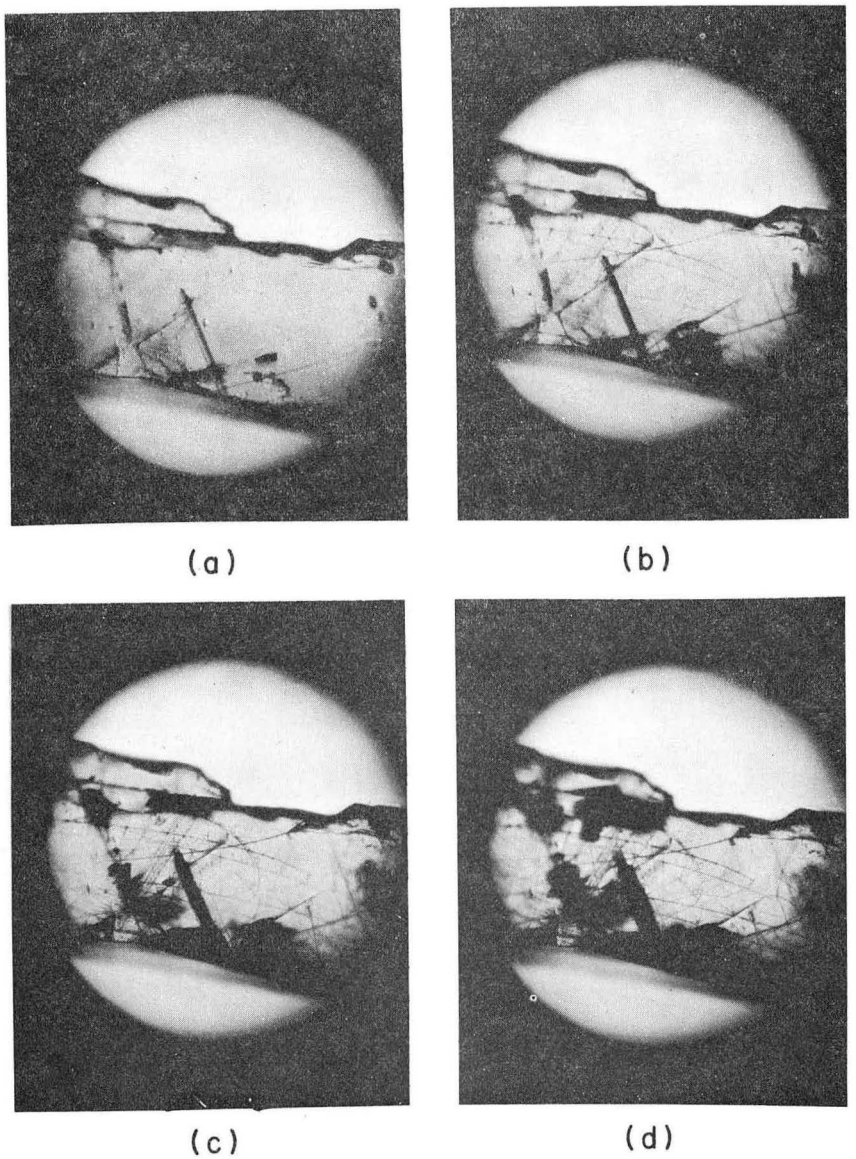

ZN-4268

Fig. 12. Photographs (a) through (f) show growth of rutile in crystal V-7. Photographs (g) and (h) show V-7 before and after transformation in transmitted light. (a) Before transformation. Note inclusions and the needle sloping down to the right. (b) Growth has begun at inclusions and at the needle. Note also the growth occurring at scratches on the surface. (c-d) Growth continues to spread from inclusions and the needle, but not from the scratches.

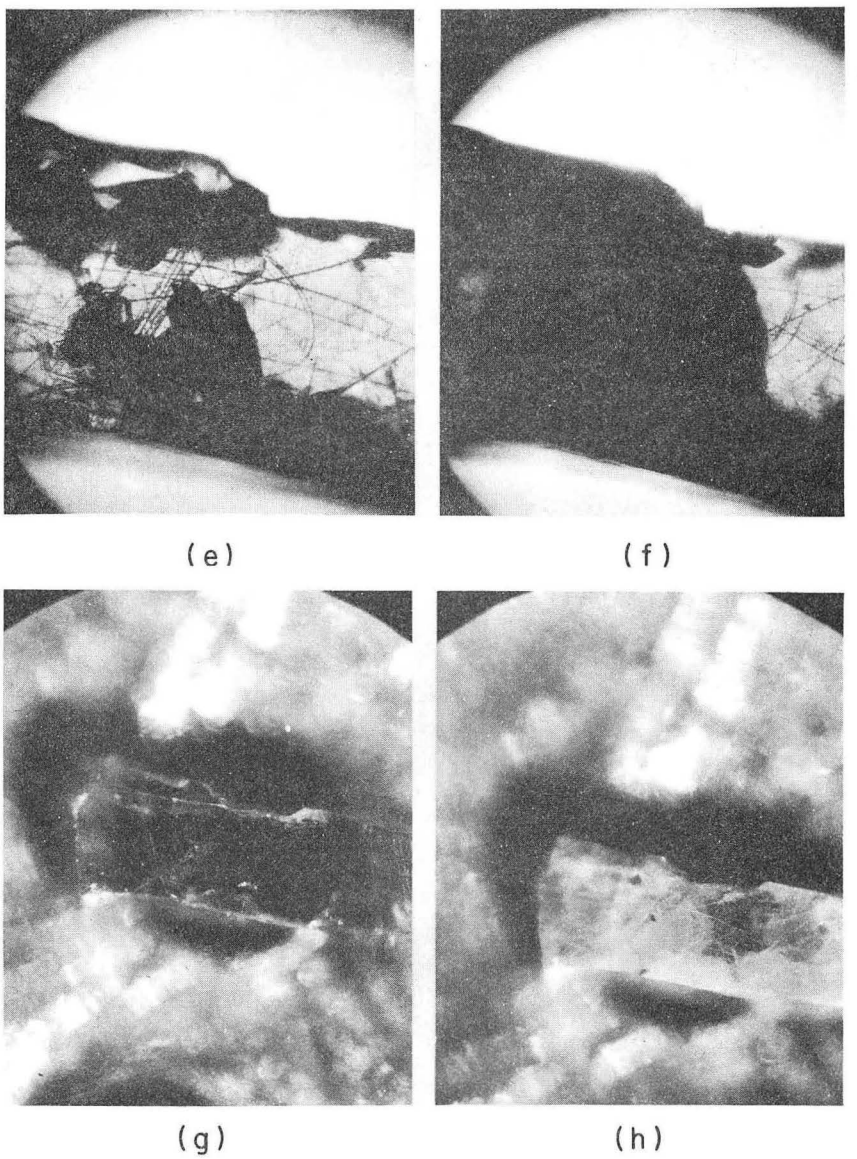

ZN-4269

Fig. 12 (continued). Photographs (e) through (f) show growth progressing until it covers almost the entire field. (g) Appearance of V-7 before transformation in transmitted light. (h) Appearance of V-7 after the transformation has proceeded as far as indicated in Fig. 12(f).

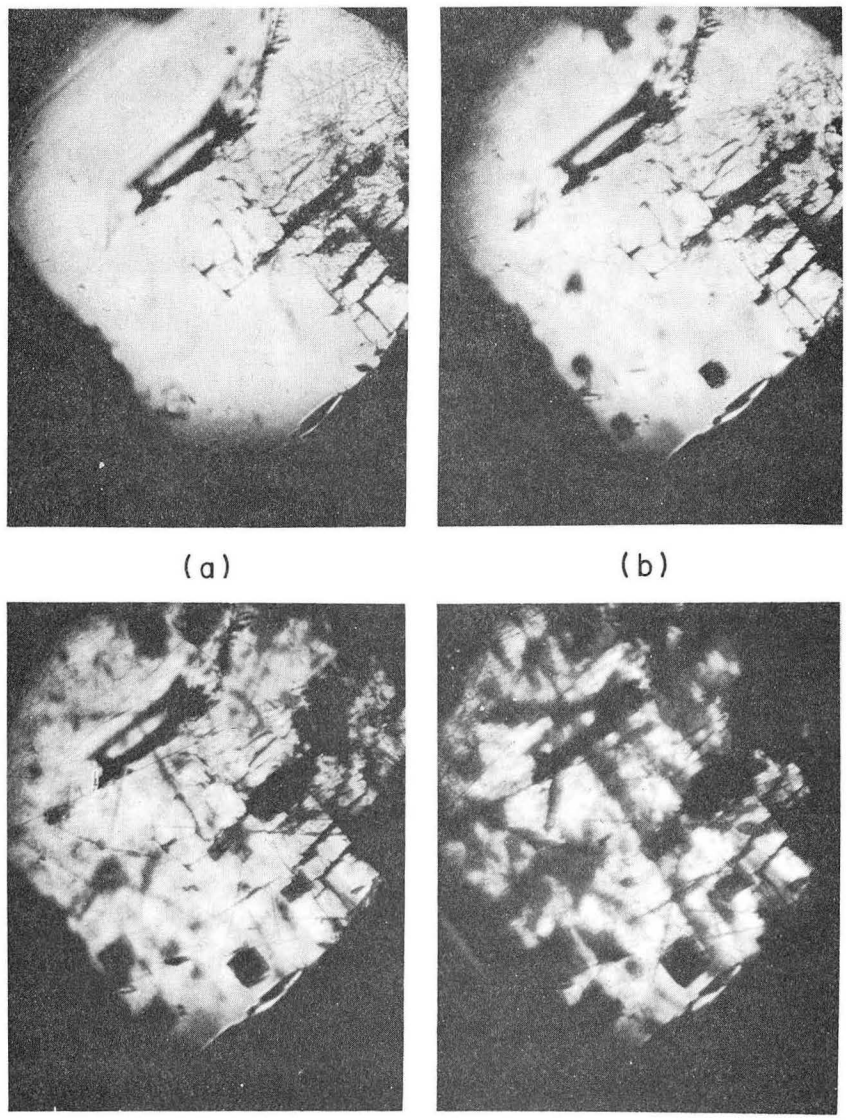

ZN-4270

Fig. 13. (a-d) Crystal V-8 showing growth at isolated points and spreading out in a rectangular front. Growth has also occurred at scratches.

Nucleation was also found to occur at discrete sites on the surface, as may be seen in crystal V8 (Fig. 13b), in which rectangular areas formed and grew readily. In general, nucleation at scratches and the formation of needles were both found to occur at temperatures 50°-75°C lower than nucleation at other sites.

Growth did not occur equally rapidly at all of the nucleated sites. The sites of rapid growth were inclusions, edges, and corners and when these centers of growth were present along with scratches and needles, they grew in exclusion of the latter. In crystals G3 and V10, the rutile growth spread across the surface in a thin layer. In Fig. 11b growth may be seen occurring simultaneously on all edges and corners while in Fig. 12b growth is seen emanating from only a few growth sites.

The orientation of the reactant sometimes affected the shape of the rutile growth, the growth being rectangular in the [001] section (Fig. 13b) while pointed in the [100] section (Figs. 12c, 12d, and 12f). The growth fronts frequently assumed geometric shapes, although at times they appeared to have irregular outlines. In crystal V10 a crack was observed that acted as a barrier to growth causing the interface to move around the crack. This behavior is illustrated in Figs. 14a and 14b.

The occurrence of nucleation at some sites at much lower temperatures than at other sites indicates varying rates of nucleus formation. The nucleation rate at scratches, interior channels, and corners thus appears to be greater than at edges and inclusions. It is therefore possible that the activation energy for nucleation at the former sites is lower. Similarly, the rate of growth is greater than that of nucleation but varies depending on the site--that for growth at scratches or needles being very low while that for growth from corners, edges, and inclusions being much higher. One expects the rate of growth at needles and scratches to be lower because of the large amount of strain energy to be overcome if growth is to occur. Similarly, at edges and corners, the rate of growth should be higher because of the larger surface energy of these sites.

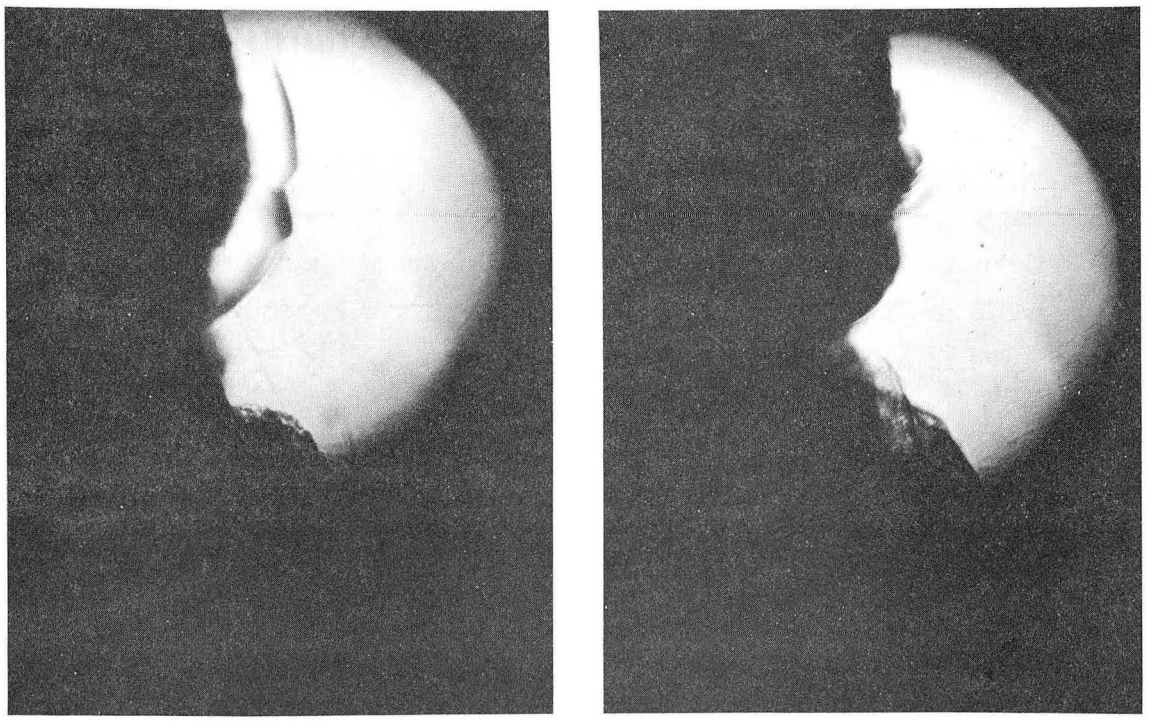

(a) (b)

ZN-4271

Fig. 14. (a, b) Growth front in crystal V-10. Note that in (b) growth has not progressed from the crack visible in (a).

2. The Origin of Rutile Needles in Anatase Crystals

The presence of bundles of rutile needles in the crystals from the Val Vals region poses the problem of their origin. Similar crystals of anatase containing residual rutile needles were described by Bauer[20] and Mügge.[21] They described a crystal from Minas Gerais, Brazil, with parallel bundle-like needles lying perpendicular to the edge formed by {112} faces, and with sagenitic groupings lying parallel to {112}. The rutile needles formed a layer 1-mm thick around a kernel of anatase, thereby indicating transformation toward the center from the surace. In a crystal from the Ural Mountains, rutile needles were found to be perpendicular to the edges formed by the intersection of the {335} faces. In yet another crystal the needles were found to lie along [001] and {110}. Since there was a lack of agreement in the orientations of the rutile needles from one crystal to the next, Mügge did not arrive at any law governing the growth of rutile in anatase.

The needles present in the crystals used in our study did not show such clearly defined orientations, although they were not entirely random. Crystal V7 showed clusters of needles lying near [100], [201], and [112], while in crystal V10 they were near [120] and [110]. Bauer and Mügge considered the growth of the rutile needles to be a clear case of paramorphism; i.e., all their samples were cases of pseudomorphs of rutile after anatase. It appears possible, however, considering the lack of more definite orientations, that a case similar to rutilated quartz may exist; in other words, the crystallization of anatase may have taken place around the already existing rutile. The lack of agreement found among the orientations is the principal argument in favor of this hypothesis. On the other hand it seems reasonable that if rutile needles had existed prior to the growth of the matrix, they would have nucleated the growth of rutile rather than anatase. Also there was a striking similarity of the needles grown in crystal G3 to the needles existing in the V series crystals. Those in G3 differed somewhat in that they did not show well-formed faces, they did not appear in mutiples, and several were not linear. The growth of needles in G3 supports the paramorphic

hypothesis and suggests that the needles formed over a geological period of time, perhaps explaining the excellent development of faces.

3. Application of Nucleation and Growth Data to the Kinetics of Powder Reactions

It was evident that an interface reaction did not set in immediately, but that in some crystals an interface reaction approximating a shrinking sphere might develop in the later stages of transformation, such as had been observed in crystal V-4. In crystal G-3 the transformation was found to spread unevenly over the entire surface before progressing to the center. However, in crystals V7 and V10 the reaction also took place by propagation from several preferred sites, spreading out three-dimensionally. Thus, it appears that the assumption of an interface reaction is not justified in the early stages of the reaction but may be valid in the later stages of reaction.

III. KINETICS OF THE POWDER REACTION

A. Introduction

Solid-state reactions are characterized by two distinct processes--nucleation of the new phase and the propagation of this new phase into the old. These reactions generally result in a sigmoid percent reaction-time (α-t) curve. The most intensely studied reactions of this type have been thermal decompositions, a broad survey of which has been made by Garner.[22] Probably an even simpler case of these reactions is the phase transformation, since nucleation and movement of the interface are not complicated by evolution of gaseous products as are decompositions and dehydrations.

The anatase-rutile transformation is characterized by the formation of a single new phase of differing volume and orientation. In Secs. I and II the reaction was shown to begin sometimes at the surface of macroscopic crystals and to progress toward the center. Since a volume shrinkage of approximately 8% occurs, a large strain energy must be overcome for nucleation to take place. This strain energy will probably be the largest contributing factor to the activation energy for nucleation, ΔG_1. After stable nuclei have formed, they continue to grow with a different activation energy for growth, ΔG_2. The relative magnitudes of these two energies determine to some degree the shape of the α-t curve. If we have $\Delta G_1 \gg \Delta G_2$, a long acceleratory period will result, assuming of course, that the rate constant for nucleation, $K_1 \ll K_2$, is the rate constant for growth. If we have $\Delta G_2 \gg \Delta G_1$, nucleation is rapid and a minimum acceleratory period results. In the case of the TiO_2 transformation the inflection point occurs at $\alpha = 0.5$, indicating an activation energy for nucleation comparable to that for growth.

In Sec. I it was indicated that in the later stages of reaction the transformation might take place as an interface reaction. The possibility of the presence of the interface reaction and the fact that commercial polycrystalline anatase exists in the shape of almost spherical

particles suggested the study of the kinetics of various commercial powders. Ideally, the kinetics of the reaction would be determined on single crystals, but no large crystals of high purity or quality were available.

Sullivan and Cole studied colloidal titania produced by a commercial process and concluded that the transformation was a first-order process with an activation energy of 100 to 110 kcal.[7] Rao prepared highly purified anatase and also found a first-order kinetic law, but a lower activation energy of 80 kcal.[8] However, none of these authors attempted to interpret their data in terms of the geometry of the crystals or to suggest a mechanism. It is generally accepted that solid-state reactions should not be considered apart from the geometry of the particles undergoing reaction and the type of nucleation which occurs.

A study of the kinetics of the transformation of several commercial powders has been carried out for two purposes: (a) We wanted to test various rate laws by assuming spherical particles (this work is covered here); and (b) wished to provide a basis for studying the effects of CuO and a reducing atmosphere on the rate of transformation; these effects are covered in Sec. IV. The rate laws used for analysis are explained in Appendix A.

B. Experimental Procedure

1. Experimental Materials

Three commercial varieties of anatase were obtained: (1) Baker and Adamson reagent TiO_2, lot R163; (2) The Glidden Company, Zopaque SD, lot 1-K-1; and (3) The American Cyanamid Co., Unitane 0-110, lot 401887. Table III gives a summary of some of the properties of these materials, and Table IV gives the results of spectrographic and chemical analyses.

Table III. Some characteristics of three commercial anatase powders.

Type	TiO_2[a] (%)	Anatase[b] (%)	Particle size (μ)	Method of preparation
B and A R163	99.0	99.0	-	-
Zopaque SD	97.3-99.2	100.0	0.05-0.25[c]	Hydrolysis of titanium sulfate solution
Unitane 0-110	99.4	99.7	0.25-0.30	Hydrolysis of titanium sulfate solution

[a]The purity of the TiO_2 samples was determined by spectrographic and chemical analyses, Table IV.

[b]The crystalline content was determined in this laboratory by x-ray analysis.

[c]A particle-size distribution performed by The Glidden Company indicated that the ZSD titania had a mean diameter of 0.14μ and that 85% of the particles had a diameter of 0.05 to 0.25 μ. Electron micrographs showed that the particles closely approximated spheres.

Table IV. Spectrographic and chemical analyses of anatase powders.

	R-163		ZSD		U-110	
	(wt-%)	mole%	(wt-%)	mole %	(wt-%)	mole %
	Spectrographic analyses of TiO_2 samples					
SiO_2	0.05[a]	0.067	0.04	0.053	0.075	0.100
Al_2O_3	0.20	0.157	0.35	0.274	---	---
MgO	0.09	0.179	0.09	0.179	0.005	0.010
CaO	0.035	0.050	0.017	0.024	0.003	0.004
FeO	---	---	0.025	0.028	---	---
SnO_2	---	---	0.01	0.015	---	---
Nb_2O_5	---	---	0.17	0.051	---	---
ZrO_2	---	---	---	---	0.08	---
BaO	---	---	---	---	0.001	---
PbO	0.005	---	0.006	---	---	---
	Chemical Analysis					
SO_3	0.018	0.018	0.014	0.014	0.075	0.075
P_2O_5	0.526	0.296	0.620	0.350	0.370	0.208

[a]These figures are the average of results obtained from two random samples of each of the indicated materials. The analyses were performed by American Spectrographic Laboratories, San Francisco, Calif.

2. Procedures

For the kinetic runs 400- to 500-mg samples were loosely packed in small platinum crucibles and heated in a tube furnace. A Pt-Pt-10% Rh thermocouple in contact with the platinum crucible was used to measure temperature. The time was measured from the instant the sample reached temperature, which was generally in the order of two minutes. The samples were air quenched after heat treatment. Material heated in platinum crucibles transformed at the same rate as that in alumina crucibles, showing that any catalytic effects were absent.

To determine whether the transformation was being initiated at the surface of each grain and/or merely at the surface of the powdered mass, powder discs were compacted at 8,000 psi and partially transformed. Analysis of the crystalline content showed 31% rutile at the surface and 27% rutile in the interior of the disc. This slight difference in amount of transformed anatase could probably be attributed to the pressure gradient in the disc, the higher pressures inducing more defects in the anatase. It was concluded from this data that the transformation was not beginning at the surface of the disc but at the surfaces of the individual grains. This conclusion was supported by the fact that the transformed disc was not observed to crack at the surface. Since the transformation involves an 8% shrinkage, severe cracking would occur in the transformed layer if the transformation were to proceed from the surface inward.

Sullivan and Cole indicated that grain growth and sintering of anatase powder occur several hundred degrees below the transformation temperatures.[7] Electron micrographs of the transformed R163 powder showed that sintering occurs during the transformation. (The electron micrographs were prepared by the Glidden Company, Pigments and Color Division, Baltimore, Maryland.) It is not clear what effect this sintering had on the kinetics of the reaction, but, certainly, if extensive sintering had occurred before the surface of the

grains were transformed, the decrease in area would have retarded the reaction rate at higher temperatures. Such an effect generally results in apparent activation energies that are lower than the true value.

The analysis of the anatase-rutile mixtures was performed according to a standard x-ray diffraction method using integrated peak heights and described fully in Klug and Alexander.[23] A rotating sample holder was used to minimize the possible orientation effects. It was not possible to avoid orientation of the long needle-like rutile crystals; thus, it was necessary to base the analysis on only the anatase content. The absence of orientation of the anatase was confirmed by agreement of the relative peak intensities with those given by the National Bureau of Standards.[24]

C. Results

Typical sigmoid curves of percent transformation (α) vs time were obtained. Figures 15a through 15c show these curves for the U-110, R163, and ZSD material. The acceleratory period was described by the exponential law (1) (See Appendix A), and was valid from $\alpha = 0.0$ to $\alpha \approx 0.50$ as shown in Fig. 16. The deceleratory period was described reasonably well by expressions (2), (3), and (4), as indicated in Figs. 17, 18, and 19. The activation-energy plots for each of these rate laws are given in Fig. 20. Table V shows a compilation of activation energies, rate constants based on the Arrhenius relationship, and the region of validity for each of the rate laws.

Differential thermal analyses were carried out on the three samples of anatase. The maximum in the exothermic peak was used as the DTA transformation temperature. Table V shows the DTA transformation temperatures for U-110, ZSD, R163, and R163 + 1% CuO.

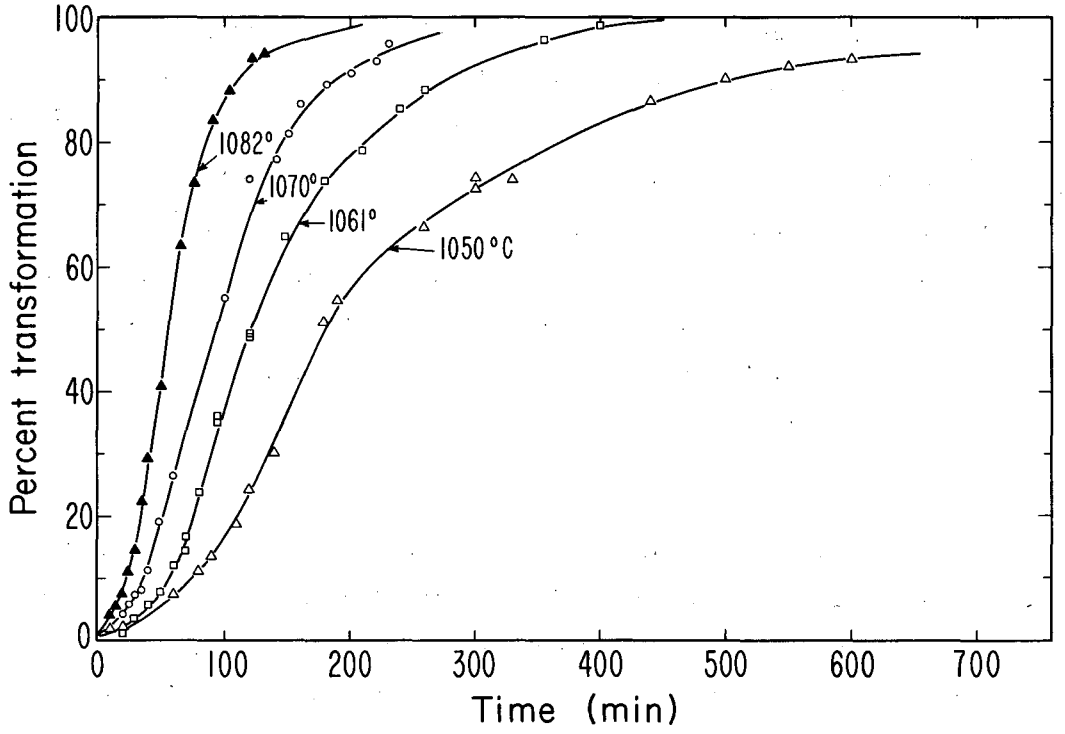

MU-33972

Fig. 15. (a) Percent transformation vs time, anatase U-110.

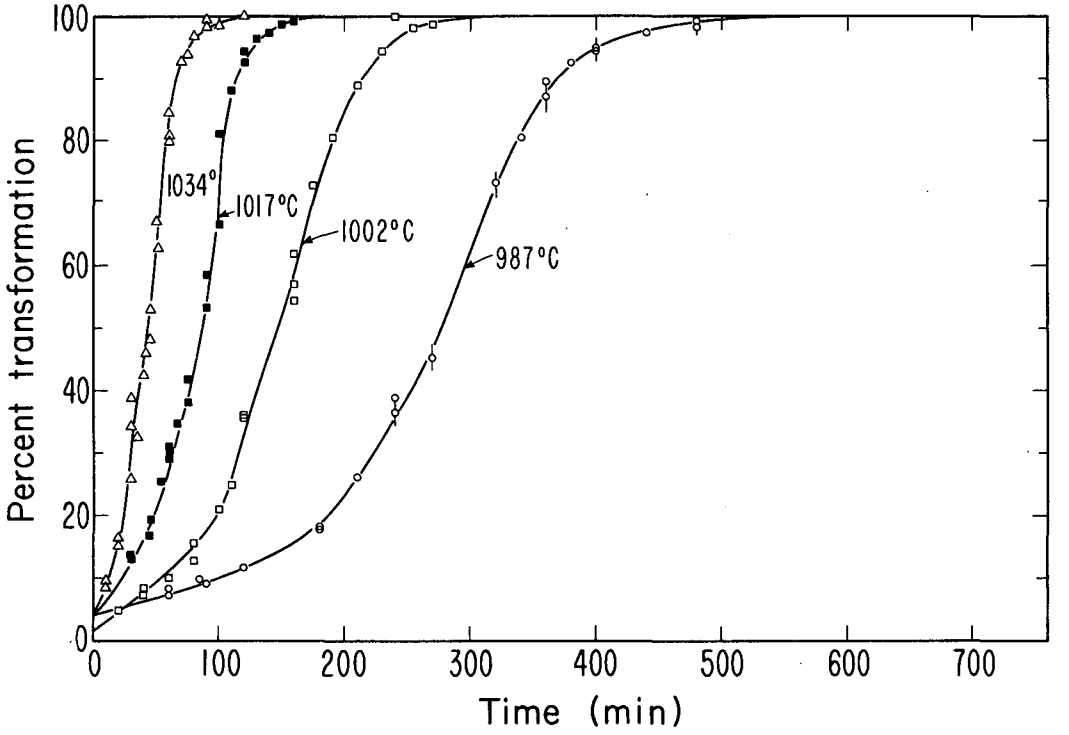

MU-33973

Fig. 15. (b) Percent transformation vs time, anatase R163.

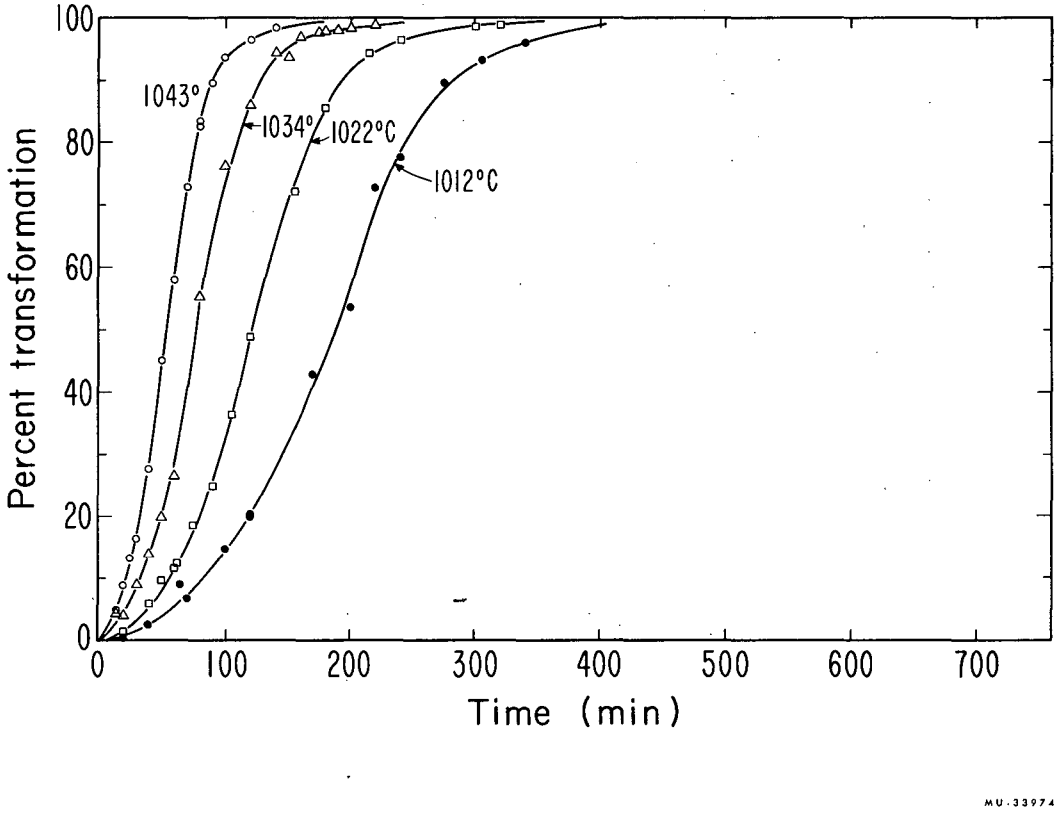

Fig. 15. (c) Percent transformation vs time, anatase ZSD.

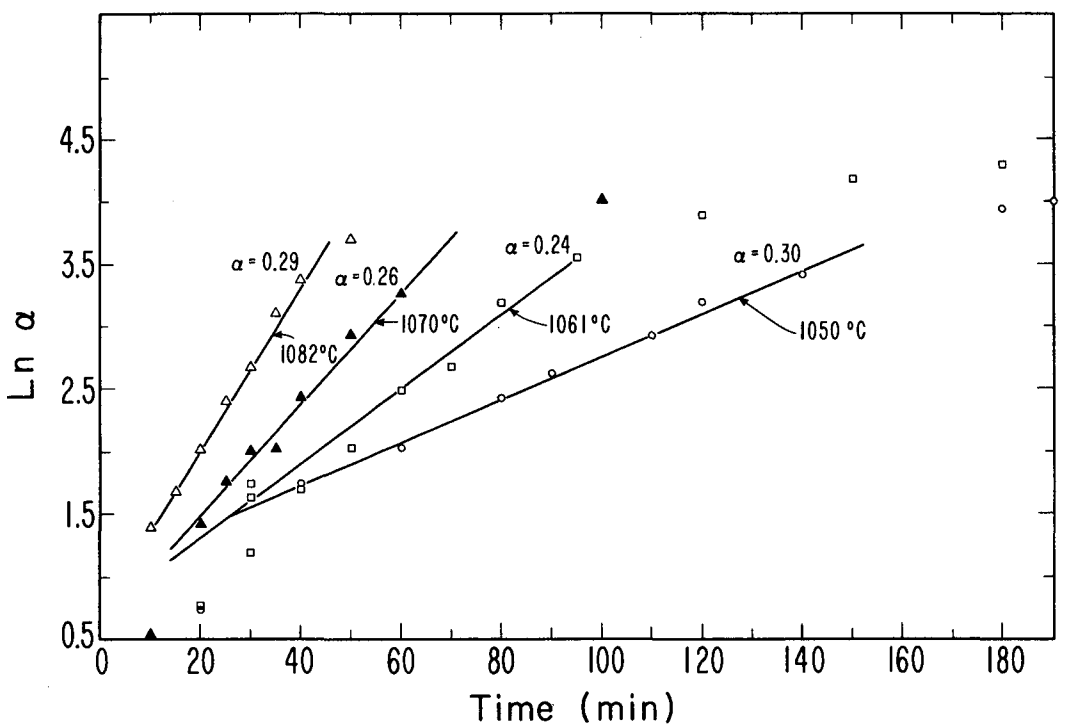

MU-33976

Fig. 16. Plot of ln α vs time, from α = 0.0 to α = 0.3, anatase U-110.

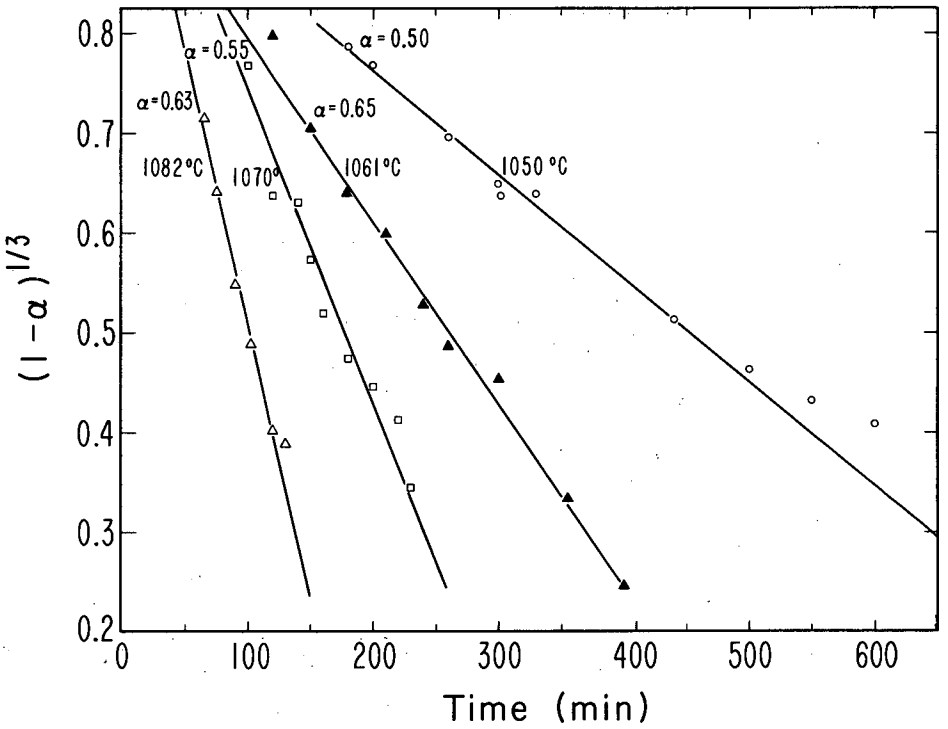

MU-33977

Fig. 17. Plot of $(1-\alpha)^{1/3}$ vs time, from $\alpha = 0.5$ to $\alpha = 1.0$, U-110.

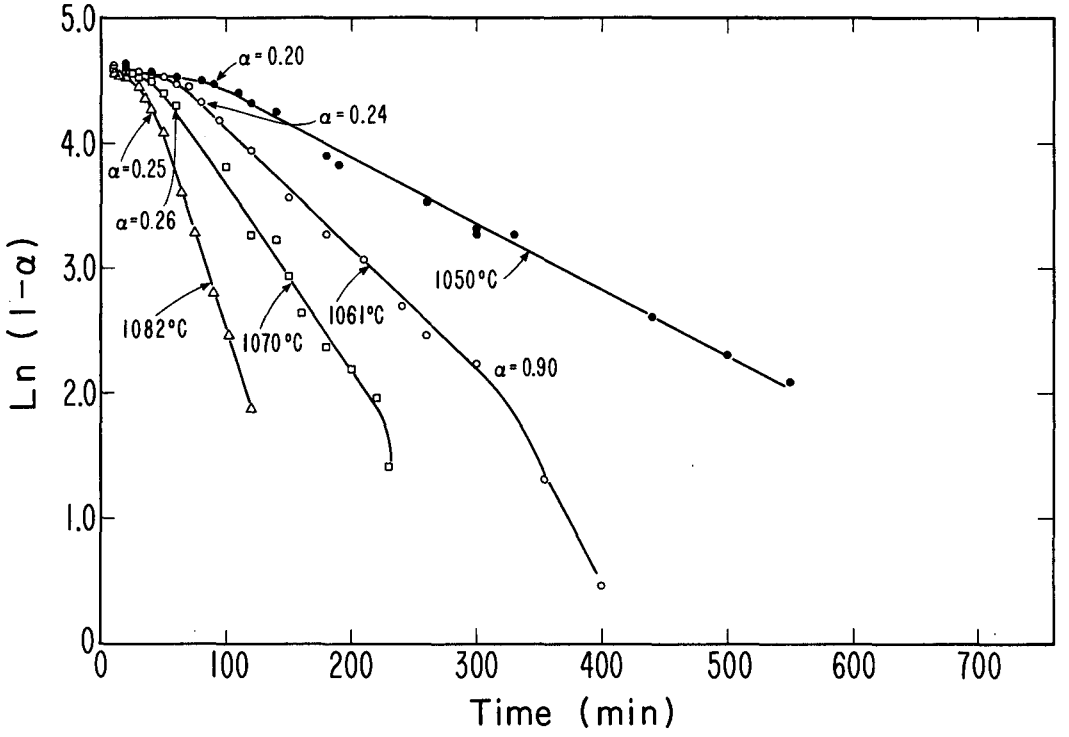

MU-33978

Fig. 18. Plot of ln(1-α) vs time from α = 0.0 to α = 1.0, U-110.

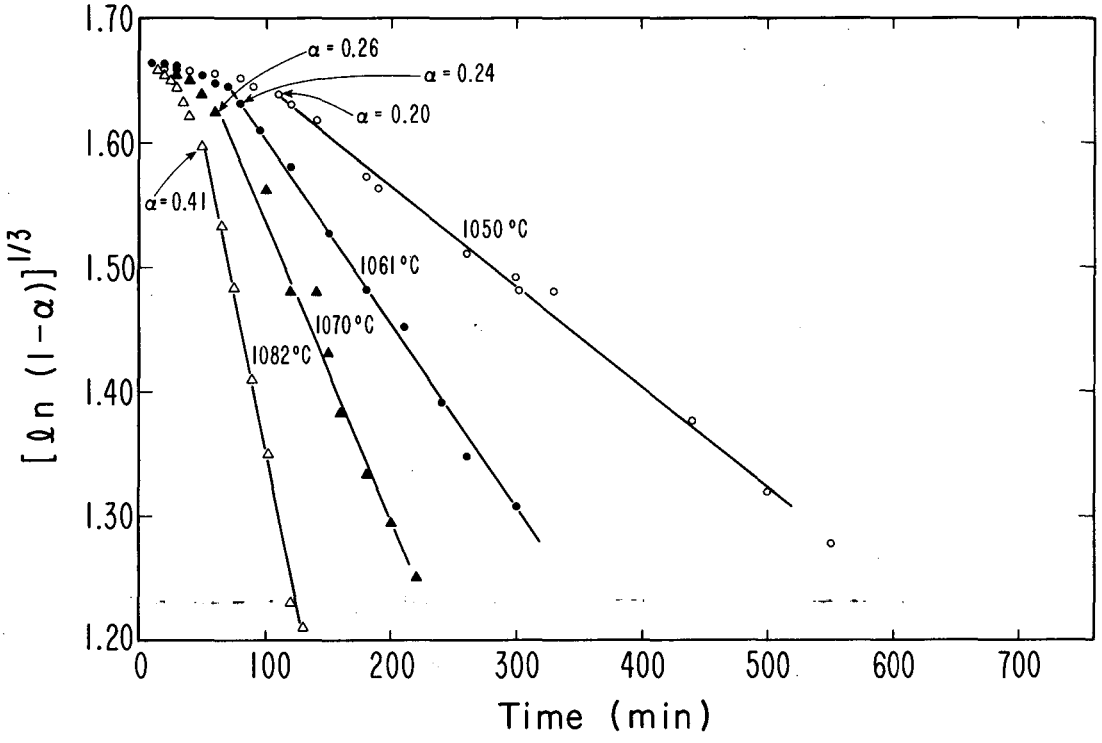

MU-33979

Fig. 19. Plot of $[\ln(1-\alpha)]^{1/3}$ vs time from $\alpha = 0.0$ to $\alpha = 1.0$, U-110.

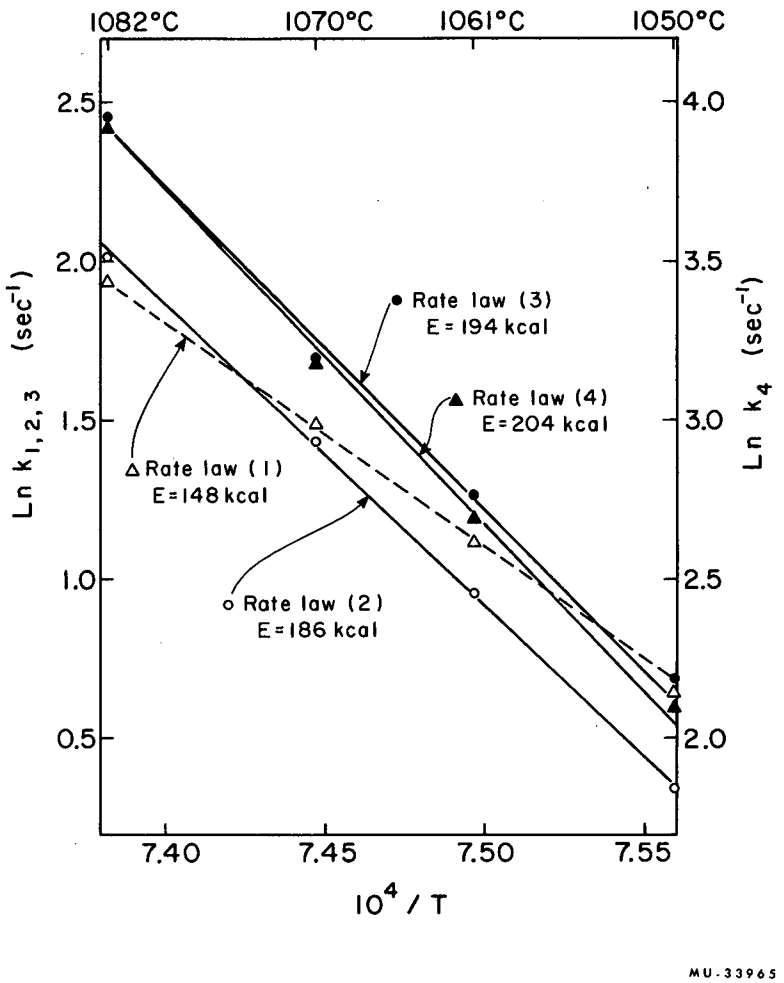

Fig. 20. Activation energy plot, ln k vs 1/T for the rate laws (1), (2), (3), and (4) for anatase U-110.

Table V. Kinetic data for the transformation of U-110, R163, ZSD and R163 + 1% CuO.

Materal	DTA transformation temperature (°C)	Expression	Region of validity	E (kcal)	A_0 (sec^{-1})
U-110	1190	(1)	0.0 - 0.5	148	7.9×10^{20}
		(2)	0.5 - 0.9	186	6.2×10^{25}
		(3)	0.3 - 0.9	194	6.2×10^{27}
		(4)	0.3 - 1.0	204	4.1×10^{29}
R163	1115	(1)	0.0 - 0.5	109	1.2×10^{15}
		(2)	0.45- 0.90	94.6	1.1×10^{12}
		(3)	0.45- 1.00	101	8.4×10^{13}
		(4)	0.70- 1.00	108	3.1×10^{14}
ZSD	1138	(1)	0.0 - 0.45	136	2.6×10^{19}
		(2)	0.40- 0.95	113	6.7×10^{14}
		(3)	---	---	---
		(4)	0.70- 0.95	116	2.4×10^{15}
		(5)	0.0 - 0.6	272	---
R163+ 1% CuO	842	(1)	0.0 - 0.60	154	4.7×10^{28}
		(2)	0.30- 0.80	180	2.2×10^{33}
		(3)	0.30- 0.90	170	8.5×10^{31}
		(4)	0.30- 0.80	180	

It does not appear possible to distinguish the correct rate law from the expressions (2), (3), and (4) since the experimental points fit each expression equally well. This is an inherent difficulty in studying powder reactions,[25] particularly those in which the geometry of the crystal is not certain and the particle size is not perfectly uniform. However, the fact that the rate expressions give an ambiguous interpretation of the mechanism does not prevent these rate curves from being used to study the effects of other variables on the rate.

The DTA transformation temperatures differ for the three materials and roughly correspond to the activation energies for growth. This correlation suggests that DTA transformation temperatures might be used to characterize the stability of different anatase samples. In Sec. IV, an attempt will be made to relate these differences in kinetics and DTA transformation temperatures to the nature and amount of impurities in the TiO_2 and thereby to the stoichiometry of the TiO_2.

IV. IMPURITY EFFECTS

A. Introduction

It has long been recognized that the rate of the anatase-rutile transformation is strongly dependent upon impurities.[4, 5, 26-28] The transformation temperature has been shown to vary from 400° to 1200°C, depending upon the method of synthesis, atmosphere, and the presence of foreign ions. Before this investigation the role these factors played in inhibiting or accelerating the transformation had not been explained. In this section a critical literature survey and the results of experimental work on the effects of CuO and hydrogen- and vacuum-reducing atmosphere on the transformation are used to show that this role is essentially that of controlling the stoichiometry of the TiO_2.

The synthesis of TiO_2 is generally carried out by high-temperature oxidation of gaseous halides,[29, 30] or by precipitation from an aqueous solution.[31, 32] The conditions for precipitation of both anatase and rutile have been summarized by Nodop.[33] Iida and Ozaki[4] studied the effect of preparation method on the transformation and concluded that a major cause for differing transformation temperatures was the degree of crystallinity of the precipitate. Czanderna et al.[6] prepared some high-purity anatase by precipitation from an ammonia solution. The low temperature of transformation exhibited by this material could be attributed to the high purity of the TiO_2, although it might have been due to the presence of the ammonia ion during precipitation. The latter conclusion is supported by the work of Knoll and Kühnhold[27] who prepared, by precipitation from ammonia solutions, some anatase which transformed at 650°C.

It has been generally found that if large quantities (> 5%) of the sulfate or phosphate ion are present, anatase is the predominant crystalline form. It was proposed by Reeves and Blouin[34] that the formation of soluble short-chain linear polymers in the sulfate solutions leads to preference for the anatase structure. The precipitate has been

found to be amorphous or of small particle size (less than 100Å) and has been found to contain as much as 9% SO_3.[7] Sullivan and Coleman[26] found that, upon heating, SO_3 is given off progressively up to the transformation region. They were unable to find any clear correlation between the rate of sulfur loss and transformation, although the removal of the last traces of S did coincide with the beginning of the transformation. It appears that the S atoms are effective in the formation of the anatase structure and as will be shown later in this section, that they help determine the stoichiometry of the TiO_2.

Conflicting data exist relating the effect of the atmosphere to the rate of transformation. Czanderna et al.[6] reported that the rate is unaffected when the transformation takes place in vacuum. Ozaki and Iida[4] found, however, that the rate was dependent on the partial pressure of oxygen, becoming slower under greater partial pressures of oxygen.

The effect of additives has been studied by numerous investigators. These effects and some experimental results obtained in this investigation are summarized in Table VI. The additives having the most pronounced inhibiting action are WO_3, and the chloride, sulfate, fluoride, and phosphate ions, in the order of increasing inhibiting effect. The additives that effectively accelerate the transformation are CuO, CoO, Li_2O, and Na_2O.

The most significant effects appear to be: (a) the accelerating action accompanying (i) the addition of CuO, CoO, and the alkali ions and (ii) the presence of a reducing atmosphere, and (b) the inhibiting effect of the sulfate, phosphate, and fluoride ions. These effects suggested to us that the defect nature of TiO_2 may be responsible for the varying rates of transformation.

The defect nature of TiO_2 is not yet fully understood. Considerable evidence for the formation of both titanium interstitials and oxygen vacancies exists. Weight-loss data as a function of oxygen pressure[35] have been used to confirm the presence of oxygen vacancies, while certain studies of the oxidation of titanium[36] and internal friction

Table VI. Compilation of data concerning the effect of impurities on transformation of anatase

Investigator	Additive	DTA T_{tr} (°C)		Remarks
Knoll and Kühnhold[27]	None	655°		Impurities added during precipitation
	≈ 0.1% NO_3^-	660		
	0.1% Cl^-	735		Inhibited transformation
	0.1% $SO_4^=$	775		Inhibited transformation
	0.1% F^-	900		Inhibited transformation
Shannon	None	1115		CuO added to the crystalline anatase as a solution of the nitrate and in all cases served to inhibit the transformation.
	0.1% CuO	1113		
	0.2%	1091		
	0.3%	1047		
	0.4%	1003		
	0.6%	932		
	0.8%	872		
	1.0%	842		
Flörke[28]		% Anatase	% Rutile	Oxides added to crystalline anatase as nitrate solution
		(After 3 days at 850°C)		
	5.0% Li_2O	0	100	Accelerator
	5.0% Na_2O	30	70	Accelerator
	5.0% K_2O	50	50	Accelerator
	5.0% CaO	90	10	---
	5.0% SrO	100	0	Inhibitor
	5.0% BaO	90	10	---
	None	80	20	---
Rao, Turner, and Honig[5]		% Anatase	% Rutile	Impurities added during precipitation
		(1 hour at 708°C)		
	None	5	95	
	5.0 at. % Zn^{++}	24	76	Inhibitor
	5.0 at. % Cl^-	51	49	Inhibitor
		(1 hour at 870°C)		
	5.0 at. % Al^{+3}	28	72	Inhibitor
	5.0 at. % $SO_4^=$	71	29	Inhibitor
	5.0 at. % $PO_4^{\equiv}$	100	0	Inhibitor

Investigator	Additive (mole%)	DTA T_{tr} (°C)				Remarks
Iida and Ozaki[4]		% Anatase	% Rutile	% Anatase	% Rutile	Impurities added to crystalline TiO_2 as solution of soluble salt
		(3 hours at 800° C)		(at 900°C)		
	None	100	0	18	82	
	Na_2O 1.0	100	0	86	14	Inhibitor
	CuO 1.0	0	100	0	100	Accelerator
	CoO 1.0	79	21	0	100	Accelerator
	NiO 1.0	97	3	0	100	Accelerator
	MnO_2 1.0	100	0	0	100	Accelerator
	Fe_2O_3 1.0	98	2	0	100	Accelerator
	Cr_2O_3 1.0	88	12	4	96	Accelerator
	MoO_3 1.0	84	16	20	80	Accelerator
	WO_3 1.0	100	0	85	15	Inhibitor
		% Rutile				
		(3 hours at 900°C)				
	Flowing O_2	52				The authors concluded that the transformation was inhibited by increased oxygen partial pressure.
	Flowing air	70				
	Flowing Ar	85				
	Vacuum	94				
	Flowing H_2	95				
	Static air	48				

studies of vacuum-reduced rutile,[37, 38] have led investigators to suggest a defect structure involving interstitial titanium ions. Electrical resistivity data[39, 40] have provided evidence for both the interstitial and vacancy mechanisms. An important factor seems to be the atmosphere in which the defects are formed. In hydrogen at all pressures,[41] and in oxygen pressures greater than 10-mm Hg, the presence of oxygen vacancies seems to be predominant.[42] At oxygen pressures less than 10-mm Hg,[42] and in $CO-CO_2$ mixtures,[40] titanium interstitials have been found. The results given by at least two authors suggest that the defect structure for vacuum-reduced and hydrogen-reduced rutile are different,[37, 41] with the interstitial mechanism predominating in vacuum-reduced TiO_2, and the oxygen vacancy mechanism predominating in hydrogen-reduced material.

In order to test the hypothesis that the defect structure of TiO_2 controls the transformation, the effect of a reducing atmosphere and of small amounts of CuO on the rate curves for R163 were studied in detail and are reported in this section. Since different defect mechanisms in vacuum and hydrogen atmosphere have been proposed, the reaction rate for R163 was also determined in vacuum. These curves were compared with those reported in Sec. III, which were obtained in air.

B. Experimental Procedure

1. Hydrogen Atmosphere and Vacuum

In order to compare the transformation kinetics in hydrogen atmospheres with those in air and with 1% CuO additions, the R163 material was heated in mixtures of H_2-N_2. The samples were brought to reaction temperature in a vacuum of 2×10^{-4}-mm Hg. These temperatures were below those at which the transformation could occur in air or vacuum. The reaction was timed from the point at which the hydrogen atmosphere was introduced and was carried out for 30 min for all samples at temperatures of 925 to 1025°C. The temperature was measured by a Pt-Pt-10% Rh thermocouple in contact with the platinum crucible. A liquid-nitrogen cold trap was used

to collect the water produced by the reduction reaction

$$TiO_2 + xH_2 = TiO_{2-x} + xH_2O.$$

Hydrogen-nitrogen atmospheres with 5%, 10%, and 20% H_2 were used. The samples were furnace-cooled in the hydrogen-nitrogen mixtures.

Samples were also heated at 1017°C under vacuum (3×10^{-4}-mm Hg obtained by an oil-diffusion pump in conjunction with a liquid-nitrogen cold trap). The specimens were first held in vacuum at 600°C for 30 min until they had outgassed; then they were placed in the hot zone of the tube furnace.

Quantitative x-ray analyses were performed in the same manner as for specimens in air. Diffuse reflectance spectra were obtained on a Cary-14 spectrophotometer to obtain a measure of the degree of reduction of TiO_2 [Figs. 21(a) and 21(b)].

2. Addition of CuO

The kinetics of transformation of the mixture R163 + 1% CuO were studied in the same way as for pure R163. The CuO was added by making a slurry with cupric-nitrate solution, and slowly drying the slurry in an oven at 95°C. The nitrate had completely decomposed to CuO at 350°C.

Differential thermal analyses were obtained for mixtures containing 0.0 to 1.0% CuO and 30% CuO. The samples were prepared in the same way as above.

Finally, diffusion couples of R163-CuO were prepared. Discs of 1-in. diam by 1/4-in. thick were pressed at 10,000 psi; these were immersed in CuO powder and heated at 800°C, the temperature range over which the transformation of the CuO-TiO_2 mixtures could be expected to go to completion. The samples were then analyzed for copper content by x-ray fluorescence at varying distances from the CuO-TiO_2 interface. The analysis was made using a General Electric XRD-3 spectrometer equipped with a pulse-height discriminator. The intensity of the CuK_a peak at $2\theta = 45.2°$ was measured at the surface

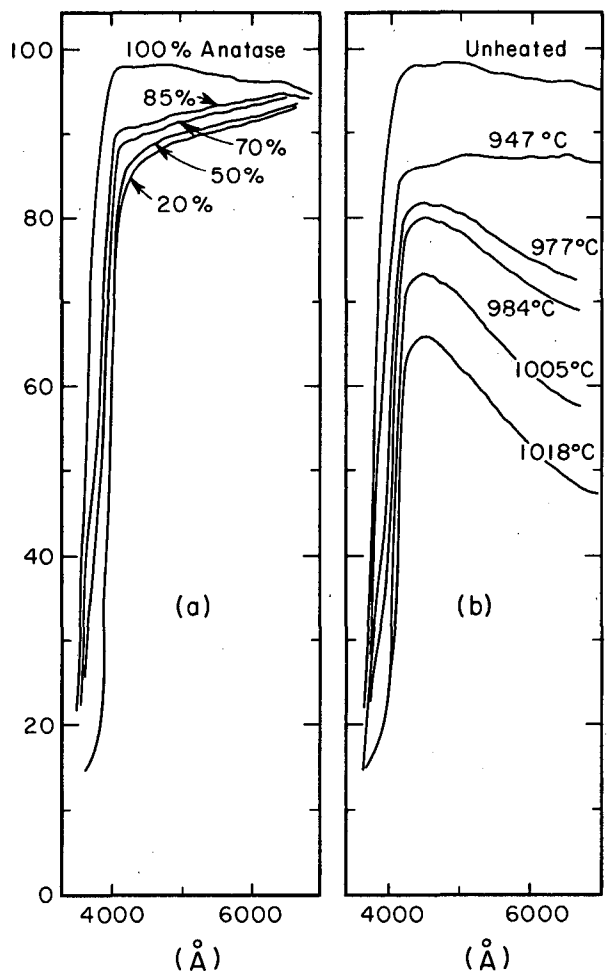

MU-33966

Fig. 21. (a) Reflectance curves for TiO_2 R163, untransformed and partially transformed in air. Curves show how the transformation affects the color of TiO_2. (b) Reflectance curves for TiO_2 R163, untransformed and partially transformed in 10% H_2-90% N_2 mixtures for 30 min at various temperatures.

of the disc. This method yielded only approximate diffusion profiles since the depth of penetration by the x-ray beam was approximately 1 mm. Standard curves were prepared with the aid of cupric nitrate-TiO_2 mixtures in which the CuO content varied from 0.0 to 1.0%.

C. Results and Discussion

One would expect the defect nature to strongly affect the chemical properties of TiO_2. In the case of the anatase-rutile transformation, oxygen vacancies would tend to accelerate the collapse of the anatase structure while formation of interstitials would tend to preserve the structure of larger volume. If one assumes that formation of oxygen vacancies is the predominant mechanism in the reduction of rutile in H_2, the accelerating effects of a hydrogen-reducing atmosphere are explained. Additionally, if one assumes diffusion of ions whose valence is less than four, and consequent substitution of these ions for Ti^{+4} ions with the formation of oxygen vacancies, the accelerating effect of Cu^{+2} and Co^{+2} becomes understandable. Conversely, substitution of ions such as S^{+6} and P^{+5} for Ti^{+4} would tend to reduce the number of vacancies and inhibit the transformation.

1. The Transformation in Hydrogen- and Vacuum- Reducing Atmosphere

In Fig. 22 the percent transformation is plotted versus the temperature of transformation for samples heated for a constant time in air, in hydrogen, and with 1% CuO additions. It is clear that the reaction is accelerated by the hydrogen atmospheres and the presence of the CuO. The degree of acceleration is proportional to the amount of hydrogen present in the atmospheres.

The samples heated in the H_2-N_2 atmospheres varied in color from light gray to a dark blue-gray, the dark color appearing in samples treated at the higher temperatures. The intensity of the color has been shown to be a measure of the reduction of the TiO_2.[43] In Fig. 23 the difference in reflectance at 6500 Å for nonreduced and reduced samples ($R_{Std.} - R_x$) is plotted versus the percent transformation. The figure shows a direct proportionality between the degree of

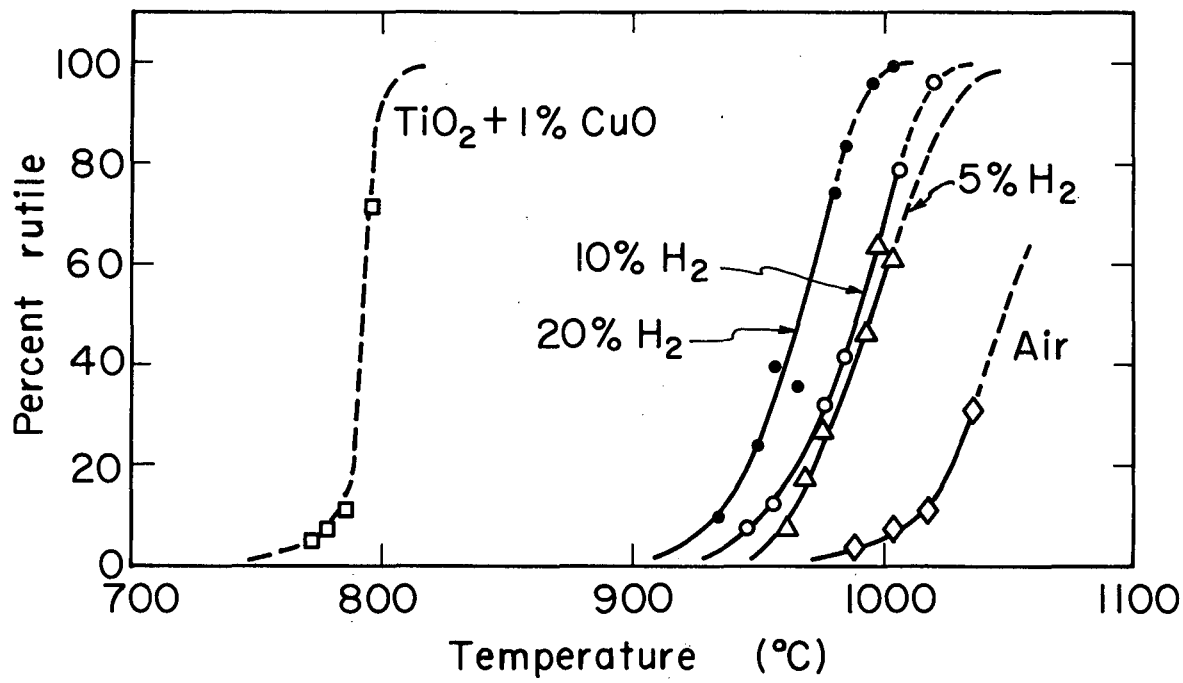

MU-33753

Fig. 22. Percent transformation vs temperature in H_2-N_2 mixtures and for TiO_2-1% CuO, transformation time ≅ 30 min., anatase R163.

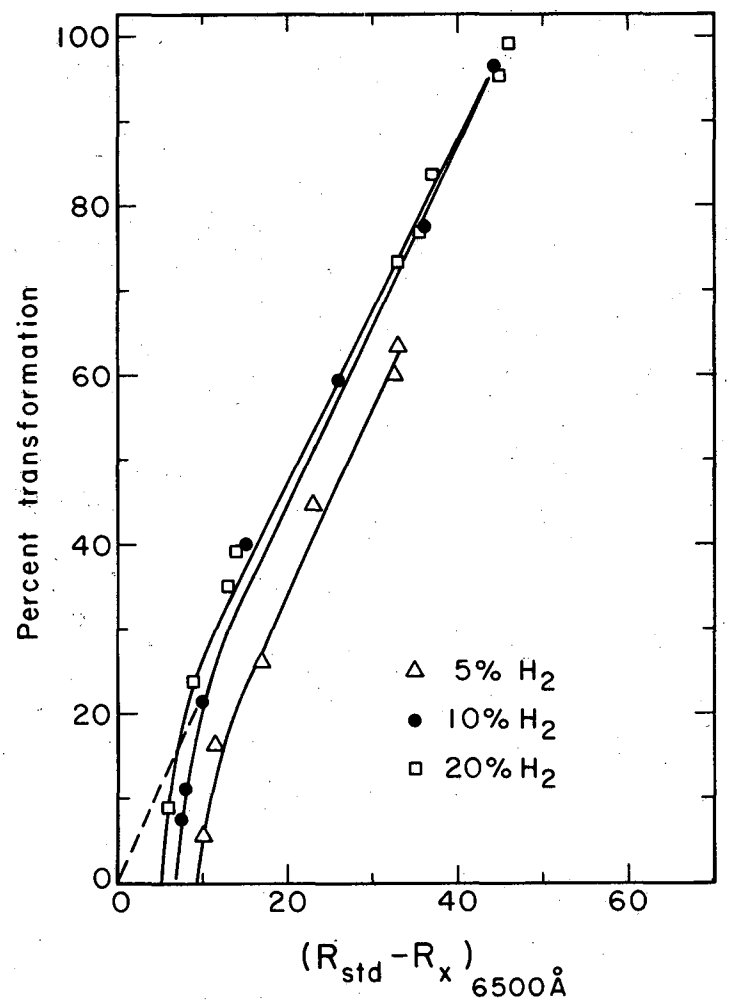

MU-33967

Fig. 23. Percent transformation vs absorption at 6500 Å ($R_{std} - R_x$), for samples of R163 heated in hydrogen-nitrogen mixtures.

reduction of TiO_2 and the amount of anatase transformed.

The accelerating effect of hydrogen could reasonably be attributed to the formation of a second phase or to the presence of oxygen vacancies. Magnéli phases of composition Ti_nO_{2n-1} where n = 4, 5, 6, 7, 8, 9, or 10 have been shown to exist in rutile[44] and might be expected to also form in anatase. The precipitates of these lower oxide phases would probably form nucleation sites for rutile. Although no second phase was detected by x-ray analysis, the precipitation of such a phase would probably be in such small quantities as to be undetectable. Straumanis[43] showed a correlation between the color of reduced rutile and composition. He indicated that the second phase appeared only when the samples had attained a dark blue color. Recent data by Blumenthal and Whitmore[45] show the homogeneity region of rutile to be even narrower than that given by Straumanis. Cell measurements showed that the homogeneity region of the rutile phase TiO_x extends from x = 2.000 to 1.991 instead of x = 2.000 to 1.983. At x = 1.991 the samples prepared by Straumanis were light gray in color. Thus, the presence of a second phase in our samples heated in H_2-N_2 mixtures appears almost certain. However, the presence of a second phase still does not rule out the presence of oxygen vacancies. From the evidence cited earlier, it is assumed that they are present and that the increase in rate of transformation in a hydrogen atmosphere is caused either by the formation of a second phase or by the presence of oxygen vacancies.

Figure 24 shows the results of runs in air and vacuum at 1017°C. The rate in vacuum follows that in air up to about 30% reaction and then begins to rapidly decrease. The defect mechanism proposed in vacuum is the formation of titanium interstitials. The reduction in rate of transformation observed in Fig. 24 strongly supports the interstitial mechanism. It might be expected that interstitials would affect both nucleation and growth rates but the experimental data do not provide any information concerning this point. Such a case is not inconsistent with the fact that the retardation does not occur until 30% transformation.

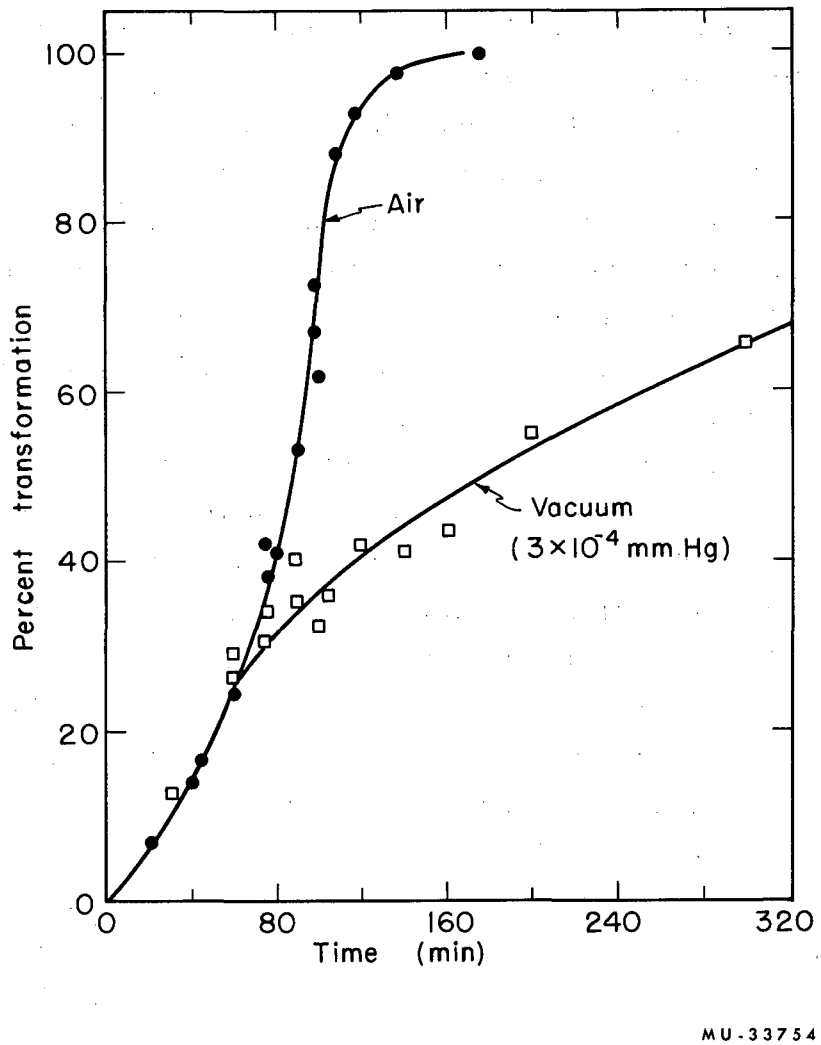

Fig. 24. Percent transformation vs time for R163 transformed in air and vacuum (3×10^{-4}-mm Hg) at 1017°C.

Since the formation of interstitials is probably also temperature activated, it might be assumed that the point at which the rate begins to decrease corresponds to the point at which the rate of formation of interstitials becomes measurable. On the other hand, it is also possible that interstitial formation inhibits the rate of growth more than the rate of nucleation; if this is true, the early stages of the transformation would not be affected, as is shown in Fig. 24.

2. Effects of CuO on the Transformation

Figure 25 shows the transformation curves for R163 + 1% CuO. Typical sigmoid curves resulted at greatly reduced temperatures. Analysis of these curves in the same manner as for pure R163 resulted in the rate constants and activation energies listed in Table V. This analysis shows that the activation energy has increased by 50 kcal. It does not seem reasonable that the activation energy for the process should increase and the transformation temperature decrease. Since the process now involves (a) reaction between CuO and TiO_2, and (b) transformation, it is evident that the kinetic expression as developed earlier is no longer valid. Probably the activation energy as measured is for a combination of processes involving transformation and diffusion of Cu^{+2} and oxygen vacancies into titania.

The DTA curves for mixtures of R163 and varying amounts of CuO show two features. First, Fig. 26 shows that the DTA transformation temperature progressively decreases from 1115° to 842°C with the amount of added CuO. Beyond 1% there is no further decrease, which suggests that some sort of surface phenomenon is occurring in which the surface of the grains is gradually being covered by CuO. Approximate calculations show that with the assumption of a monomolecular layer of the oxide, 1% CuO would completely cover the surface.

Secondly, it can be seen from Fig. 27 that the temperature interval--over which the reaction occurs--decreased with the amount of CuO. This interval is generally an indication of the apparent activation energy for the process. Thus it can be concluded that the activation energy gradually increases with the amount of added CuO.

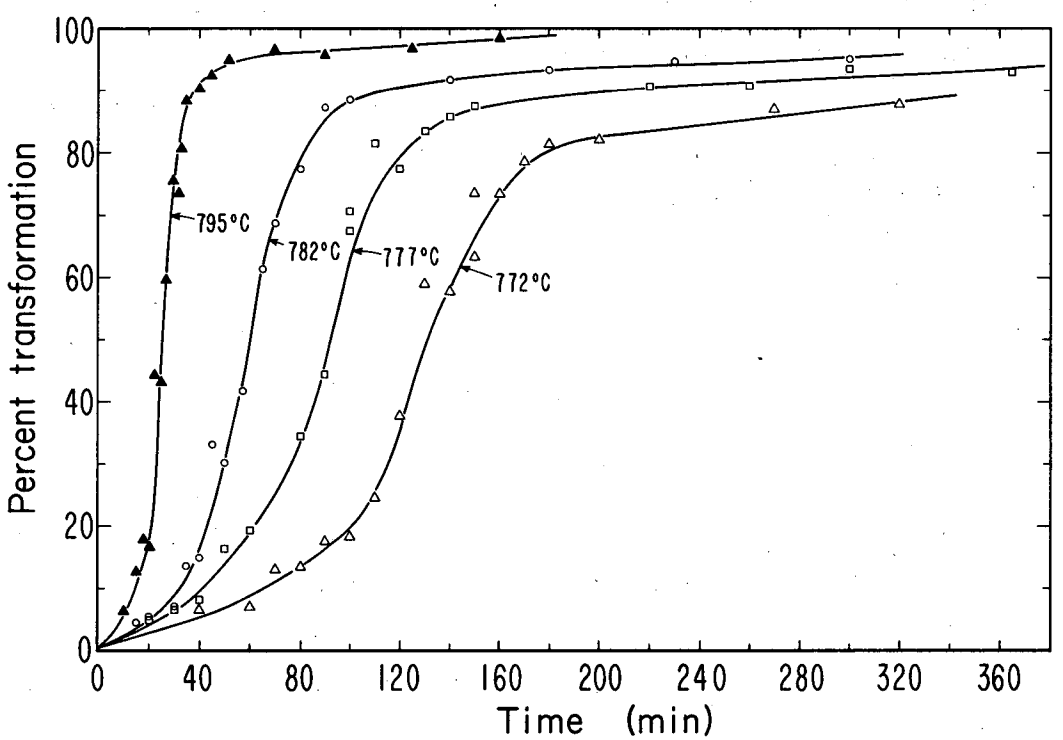

MU-33971

Fig. 25. Percent transformation vs time for mixtures of R163 and 1% CuO.

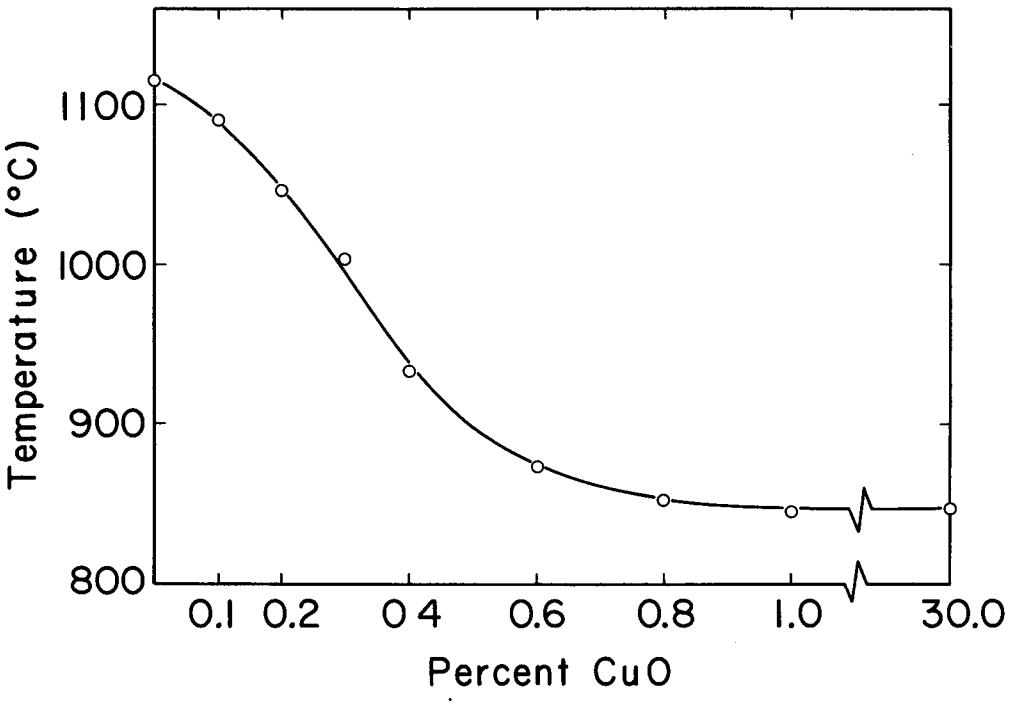

MU-33968

Fig. 26. DTA transformation temperature vs percent CuO in mixtures of R163-CuO.

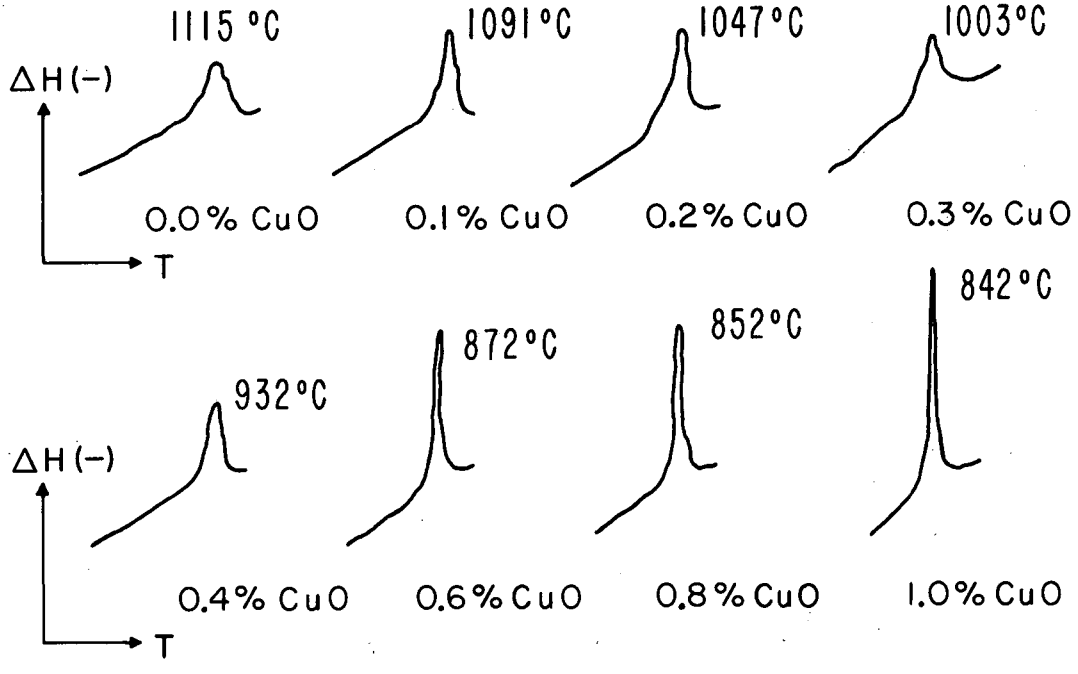

MU-33969

Fig. 27. DTA curves showing the exothermic peak caused by the anatase-rutile transformation for various mixtures of R163-CuO; heating rate = 12°C/min.

This conclusion further supports the results with the R163-1% CuO mixtures in which the apparent activation energy was 175 kcal/mole.

The accelerating effect of the CuO might be caused by one or more of the following reactions: (a) a new TiO_2-CuO phase forming with possible enhancement of the nucleation rate; (b) oxidation of a cuprous compound formed during the decomposition of cupric nitrate; or (c) the formation of a solid solution.

Taylor[46] found no evidence of any compound formation in mixtures of CuO and TiO_2 samples quenched from 1000° C. No traces of a second phase were shown in x-ray analyses of the mixtures of 1% and 30% CuO with R163. This data, however, does not preclude the possibility of a high-temperature phase similar to that present in the CuO-Al_2O_3 system,[47] but it is unlikely that such a phase would decompose so rapidly on quenching as to completely prevent its detection.

The CuO was added in the form of $Cu(NO_3)_2 \cdot 3\ H_2O$. The decomposition of the trihydrate has been found to go through several stages. The formation of an oxynitrate $Cu(NO_3)_2 \cdot 3\ Cu(OH)_2$ was reported to occur at 170° to 230°C with decomposition to CuO at 300°C.[48] Although the presence of Cu_2O was reported by Lecuir,[48] diffraction analysis performed by us on the samples of the trihydrate decomposed above 350°C showed no traces of any crystalline material other than CuO. Thus, the possibility of oxidation of a cuprous compound at the transformation temperatures seems remote.

No reference to formation of a solid solution of CuO in TiO_2 was found in the literature. To test the possibility that solid solutions were nevertheless formed, the diffusion couple was prepared. The diffusion profile is shown in Fig. 28, in which the Cu content and percent transformation are plotted as functions of the distance from the CuO-TiO_2 interface. Solid solution of Cu^{++} in TiO_2 at temperatures of 800 to 880°C occurs with the maximum concentration of copper apparently 0.2 to 0.3 weight-% or approximately 0.25 to 0.38 mole %. The formation of solid solution precedes the transformation and clearly causes the acceleration observed in Fig. 22. The mechanism through

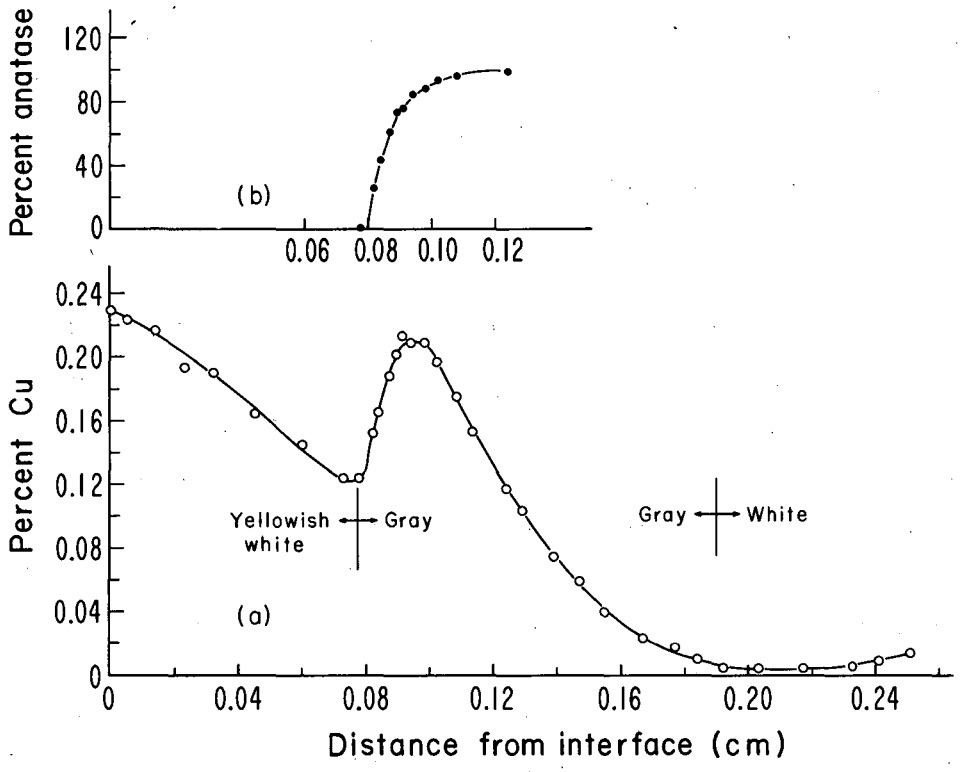

MU-33970

Fig. 28. (a) Percent copper vs distance from the $CuO-TiO_2$ interface. The sample was a pressed disc of R163 heated in CuO powder for 6 h at 880°C. (b) Percent anatase vs distance from the $CuO-TiO_2$ interface.

which the rate of transformation increases is, however, open to several interpretations. The copper ions dissolved in TiO_2 must occupy either (a) substitutional, or (b) interstitial sites. Case (a) implies the formation of oxygen vacancies or an increase in titanium interstitials to preserve electrical neutrality, while (b) indicates a reduction in oxygen vacancy or titanium interstitial concentration. It would seem that only (a) with the formation of oxygen vacancies is likely to promote the transformation. Any increase in the number of interstitial ions should reduce the rate of transformation. Although (b) involves a decrease in titanium interstitials, this decrease is more than compensated for by the copper interstitials. We concluded that solid solution of copper with the concomitant formation of oxygen vacancies is the cause of the accelerated transformation, although this conclusion was subject to the same consideration as the reduction of TiO_2 in hydrogen, namely, that formation of oxygen vacancies could lead to the formation of a second $Ti_n O_{2n-1}$ phase. The single-phase region in rutile extends down to $TiO_{1.991}$. We assumed that the single-phase region in $Ti_{1-x} Cu_x O_{2-2x}$ extends to the same oxygen content. Since the maximum amount of copper dissolved corresponds to $Ti_{0.996} Cu_{0.004} O_{1.992}$, the possibility of a second phase was rejected.

A curious feature of the diffusion profile is the increase in copper concentration as the amount of anatase increases. This may indicate a higher solubility and/or diffusivity of Cu^{+2} in anatase. Such a result is not surprising when one considers the expanded and more defective anatase structure. A significant point is that diffusion is evidently proceeding against a positive concentration gradient. The existence of this solid solubility region points to the probable formation of oxygen vacancies at the level of 1.2×10^{21} vacancies per mole.

Ionic size is important consideration in solid-solution formation. Wells[17] lists the ionic radii of Ti^{+4} and Cu^{+} as 0.68 Å and 0.96 Å, respectively, but fails to give a value of Cu^{+2}. An estimate of 0.57 Å was made from nearest-neighbor distances in a number of cupric

compounds as listed in Table VII. Thus, on the basis of ionic radius, the assumption of solid solubility appears valid. These data, interpreted in conjunction with the rates in hydrogen and vacuum, strongly suggest the formation of solid solution and the resulting oxygen vacancies as the most important factor in the accelerating effect of CuO.

3. General Considerations of Impurity Effects

It is interesting to compare the DTA transformation temperatures for the three varieties of TiO_2 already studied, R163, ZSD, and U-110, in light of the impurity contents shown in Table IV. By assuming that only those impurity ions of the proper size could form solid solution (Al^{+3}, Mg^{+2}, Ca^{+2}, Fe^{+2} Nb^{+5}, S^{+6}, and P^{+5}), and that ions of valence less than four increase the vacancy concentration while those of valence greater than four reduce the vacancy concentration, it is possible to arrive at a speculative estimate of the change in vacancy content from the equilibrium value. No studies of the equilibrium concentration of vacancies in anatase have been made but Buessem and Butler,[49] by assuming reaction (1), were able to determine the vacancy concentration in rutile by measuring the change in weight as a function of the oxygen pressure:

$$2Ti^{+4} + O^{=} = (AV) + 2\ Ti^{+3} + \frac{1}{2}\ O_2(g). \qquad (1)$$

Table VIII shows the equilibrium number of vacancies in rutile in the temperature range used for the study of U-110, ZSD, and R163, as calculated in Appendix B. The vacancy concentration in anatase would not be identical to that in rutile, but because of similarities in bond strength and coordination these concentrations should be of the same order of magnitude. Table IX shows the correlation between the change in vacancy concentration from the equilibrium value and the DTA transformation temperature. The change in vacancy concentration caused by the nature of the impurities is significant in comparison to the equilibrium value and should be expected to affect the transformation rate.

Table VII. Interionic distances in some cupric compounds.

Compound	Distance[a] between	Cu^{+2}	and	ionic radius
$CuCl_2$	4 Cl	2.30		0.58
$CuBr_2$	4 Br	2.40		0.48
$CuCl_2 \cdot 2\ H_2O$	2 Cl	2.28		0.56
	2 O	1.93		0.61
$CuCsCl_3$	4 Cl	2.30		0.58
$K_2CuCl_4 \cdot 2\ H_2O$	2 O	1.97		0.55
	2 Cl	2.32		0.60
CuF_2 (distorted rutile structure)	2 F	1.93		0.57
TiO_2 (rutile)	2 O	1.946		0.62

Average: $r_{Cu^{++}} = 0.57$ Å

[a]Interatomic distances taken from Wells.[17]

Table VIII. Equilibrium concentration of vacancies in rutile.[a,b]

Temperature (°C)	K_{exp} ($atm^{1/2}$)	n_{AV} $\times 10^{-3}$	N_{AV} (vacancies/mole)$\times 10^{21}$
950	7.26×10^{-8}	3.4	2.1
1000	2.39×10^{-7}	5.1	3.1
1050	9.43×10^{-7}	8.1	4.8

[a]See Appendix B for calculations.

[b]From reference 49.

Table IX. Transformation temperature, change in vacancy concentration, and activation energy for various samples of anatase.

Material	DTA T_{tr} (°C)	Change in vacancy concentration per mole from the equilibrium concentration ($\times 10^{21}$)	Activation energy (kcal/mole)
U-110	1190	-2.0	190
ZSD	1138	+1.8	115
R163	1115	+1.6	100
R163+1% CuO	842	+7.7	---

Although the data obtained in this study indicate that the nature of the impurities and the transformation environment to a large degree control the transformation temperature, it would also seem reasonable to expect the total impurity level to affect the transformation temperature and the activation energy. Table X shows that a high level of impurities seems to raise the transformation temperature. The specimens prepared by both Rao[8] and Knoll and Kühnhold[27] in ammonia solutions transform in the range 600° to 700°C, while most TiO_2 precipitated from sulfate solutions seems to transform in the range 800° to 1000°C. Rao's TiO_2 was spectroscopically pure, while Knoll and Kühnhold did not provide any indication of the purity of their material. It is not clear why the effect of the ammonia solutions is to allow a low transformation temperature. Impurities entering into solid solution could easily occupy the large interstitial positions in the anatase structure and would by stuffing the structure, tend to prevent collapse of the structure. Besides stuffing the structure, substitutional cations of valence greater than four would tend to decrease the oxygen-vacancy concentration. Thus, low impurity levels tend to favor a low transformation temperature and a low activation energy. However, even if the impurity level is low, the transformation temperature may still be high if the impurities are those which tend to reduce the vacancy concentration.

Probably the variation in transformation rate among different samples of anatase is largely a result of a change in the activation energy. The activation energy can be thought of as arising from the strain energy developed during deformation of the oxygen close-packed structure and from the energy necessary to break the Ti-O bonds. The effect of the addition of impurities would be to increase the strain energy unless these impurities were such as to create oxygen vacancies. In the latter case one would expect the strain energy to be decreased. The presence of the oxygen vacancies would also decrease the number of Ti-O bonds which must be broken. The effects of impurities can be summarized:

Table X. Transformation characteristics of anatase preparations

Investigator	Sample	Approx. Percent TiO_2	DTA T_{tr}	Temp. of 50% reaction in 60 min	Activation energy
Shannon	U-110	99.6	1190°C[a]	1080	190 ± 10
	ZSD	99.0	1138	1040	115 ± 10
	R163	99.2	1115	1025	100 ± 10
	R163 + 1% CuO	98.2	842	782	
Rao[8]		99.9	≈650[b]	700	80 ± 10
Sullivan and Cole[7]		99.8	900[c]	790	105 ± 5
Sullivan and Coleman[26]	1	99.6	---	840	66
	2	99.6	---	850	85
	3	99.6	---	840	76
	4	99.6	---	975	41
Kuhnhold and Knoll[27]	Tetraethyl[d] ester	?	655	---	---
	NO_3^-		660	---	---
	Cl^-		735	---	---
	$SO_4^=$		775	---	---
	F^-		900	---	---

[a]heating rate = 12°C/min

[b]heating rate = 12.5°C/min

[c]heating rate = 5°C/min

[d]Precipitated from ammonia solution with the presence of the indicated ions. Analysis of the anhydrous precipitate showed approximately 0.1% of the anions shown.

(a) Those impurities which enter interstitial positions or substitutional ions larger than Ti^{+4} increase the strain energy, unless by creating anion vacancies they reduce the number of Ti-O bonds which must be broken.

(b) The impurities that form substitutional solid solution and create anion vacancies reduce the strain energy and the number of Ti-O bonds that must be ruptured.

When the transformation takes place in a reducing atmosphere or in contact with impurities that go into solid solution, the process is complex. The following steps may take place:

	Rate
(1) Formation of vacancies at the surface	R_v
(2) Nucleation of the rutile phase	R_{nucl}
(3) Diffusion of the vacancies toward the interior of the crystal	R_d
(4) Growth of the nucleated rutile crystals	R_g

If we assume $R_v \gg R_d$, it is possible that the vacancies could accumulate at the surface and eventually nucleate micropores which would tend to reduce the activation energy for transformation or increase the number of possible sites of nucleation. Seitz[50] has stated that (a) vacancies will condense at spherical voids or inclusions in metals containing a volume of $\approx$ 1000 lattice sites if $\frac{N_v}{N_{v_o}} \geqslant 2$, and (b) in a perfect crystal vacancies may condense to form voids if $\frac{N_v}{N_{v_o}} \geqslant 100$. ($N_v$ = number of vacancies present per cm^3; N_{v_o} = equilibrium number of vacancies per cm^3.) If it is accepted that the rate of nucleation is increased by the presence of vacancies, whether or not the rate of growth R_g is increased depends on R_d. The diffusion couple showed that the diffusion of Cu^{++} proceeded ahead of the transformation so that $R_d > R_g$. Such a condition should increase the rate of growth, this was observed.

If $R_v < R_d$ the vacancies would have diffused rapidly throughout the entire specimen, probably not nucleating voids at the surface. In this case one would not expect such a radical change in the nucleation rate as was observed.

From the preceding considerations, the probable sequence of events in the CuO or H_2 accelerated transformation is as follows:

(1) Vacancies (with or without voids) form via diffusion of Cu^{++} or the reaction of H_2 with TiO_2. Precipitation of a second phase might be possible when reduction by H_2 occurs.

(2) Rutile nucleates and vacancies diffuse toward the interior of the crystal. Rutile nucleation would be promoted by the formation of a second phase.

(3) Rutile grows and vacancies diffuse further.

The corresponding sequence of events in vacuum is:

(1) nucleation of rutile and formation of titanium interstitials--possible reduced rate of nucleation of rutile;

(2) growth of rutile and diffusion of titanium interstitials toward the interior of the crystal;

(3) reduced rate of growth of rutile.

GENERAL SUMMARY

In Sec. I the anatase-rutile transformation was found to be a case of intermediate topotaxy. Pole figures derived from a study of the orientation of the rutile phase allowed an interpretation of the mechanism of the transformation on a microscopic scale. The apparently diffusionless transformation was shown to involve considerable distortion of the original structure. The pseudo-close-packed planes essentially retain their original spacing while undergoing distortion within the planes. The pseudo-hexagonal planes (112) in anatase are extremely distorted and must undergo a large degree of movement to attain the more perfect hexagonal arrangement of the (200) planes in rutile. The mechanism for the structural change is a cooperative movement of the oxygen and titanium ions in which three-fourths of the titanium ions break two Ti-O bonds in the process of reaching their new sites, while the remaining fourth retain their original six neighbors.

The nucleation and growth of rutile as observed under a hot stage microscope was described in Sec. II. The nucleation sites were principally inclusions and edges and corners of the crystal. Growth propagated both over the surface and three dimensionally from a single point in the crystal. It was concluded that an interface reaction might occur in the later stages of transformation.

The transformation kinetics of three commercial TiO_2 powders were determined in Sec. III. Sigmoid-transformation rate curves were obtained and these were interpreted in terms of a nucleation-growth process in which the activation energy for nucleation was comparable to that for growth. Several rate laws were successfully applied to the transformation-time curves but no clear interpretation of the mechanism could be derived from the rate laws. Activation energies for the three powders were 100, 115, and 190 kcal/mole.

In Sec. IV the effects of impurities and of the transformation environment were described. In this study small amounts of CuO and a hydrogen atmosphere were found to accelerate the transformation while a vacuum of 3×10^{-4}-mm Hg inhibited the transformation beyond

$\alpha = 0.30$. Copper oxide was found to go into solid solution with TiO_2 up to 0.2 to 0.3 weight %. The suggested mechanism through which the rate changes occurred concerns changes in the TiO_2 defect concentration. The following are proposed:

(1) The presence of a hydrogen atmosphere increases the vacancy concentration, thereby facilitating the collapse of the anatase structure. However, the increased rate of transformation can also be attributed to the formation of a second Ti_nO_{2n-1} phase precipitate. Precipitation of such a phase could provide nucleation centers for rutile.

(2) Substitutional solid solution of CuO increases the oxygen-vacancy concentration and acts in a similar manner to hydrogen. The amount of dissolved CuO appears to be too small to bring about the formation of a second phase.

(3) In a vacuum of 3×10^{-4}-mm Hg, interstitial titanium ions form and, by means of a structure stuffing effect, reduce the rate of transformation.

The over-all effect of impurities appears to be twofold. First, the total impurity content affects the transformation through the structure stuffing effect. Large quantities of most impurities raise the transformation temperature, probably by increasing the activation energy. Secondly, the nature of the impurities appears to control the stoichiometry of the TiO_2. It is assumed that the oxygen-vacancy defect mechanism is operative. Ions of valence less than four and of small ionic radius which can substitutionally enter the structure, e.g., Cu^{++}, Co^{++} or Li^{+}, would increase the oxygen-vacancy concentration. This increase in vacancy concentration presumably reduces the strain energy that must be overcome before collapse of the structure can occur. Ions of valence greater than four, e.g., P^{+5} and S^{+6}, would correspondingly reduce the oxygen-vacancy concentration and the rate of transformation. Similarly, substitution of two fluoride ions for an oxygen ion would reduce the number of oxygen vacancies and inhibit the transformation.

ACKNOWLEDGMENTS

The author wishes to thank J. A. Pask and A. Pabst for many helpful discussions concerning this work. Special thanks are extended to Professor Pabst and the Department of Geology and Geophysics for use of the x-ray equipment mentioned in Sec. I. Appreciation is also expressed to C. R. McKibben and A. C. Dreshfield of the Glidden Co., Baltimore, Md. for providing the particle size analysis on the ZSD material and electron micrographs of the transformed samples.

This work was done under the auspices of the U. S. Atomic Energy Commission.

APPENDICES

A. Rate Laws for Some Solid State Transformations

Jacobs and Tompkins[25] have treated nucleation and growth in solid phases extensively. They used several laws for nucleation and considered the growth of one, two, and three-dimensional nuclei in both single crystals and polycrystalline aggregates. They reviewed the development of a series of expressions that have been used to explain the course of numerous reactions. These expressions, however, are seldom unambiguous and commonly several expressions fit the data equally well. The mechanism of the reaction is, therefore, rarely unequivocally determined using these equations and supplemental information is usually required.

Jacobs and Tompkins explained the general method of formulating rate expressions as follows:

The volume of the reacted material is

$$V(t, y) = \int_0^t v(t, y) \left.\frac{dN}{dt}\right]_{t = y} dy,$$

where $V(t, y)$ is the volume of a single nucleus nucleated at time $t = y$ and growing up to time $t = t$, and $\frac{dN}{dt}$ is the rate of nucleation. Then,

$$\alpha = \frac{V(t, y)}{V_o},$$

where V_o is the original volume of reactant.

For the three types of anatase studied, the acceleratory period is described reasonably well by an exponential law

$$\ln \alpha = k_3 t + c. \qquad (1)$$

This law is based on the assumption of one-dimensional, linear, branching nuclei and a constant growth rate. The concept of these branching chains of nuclei is not explicit but is expressed in the rate of nucleation by

$$\frac{dN}{dt} = K_1 N_o + K_3 N,$$

where K_1 is the nucleation-rate constant, K_3 is the branching coefficient, N_o is the number of possible nucleation sites, and N is the number of active nuclei.

The fact that the acceleratory period is so long ($\alpha = 0.0 \rightarrow \approx 0.5$) indicates that the activation energy for nucleation is of the same order of magnitude as that for growth. Previous considerations of the change in unit-cell dimensions and the disruption that must take place on reorientation indicate this conclusion is justified.

Numerous expressions adequately describe the deceleratory period, thus precluding an exact analysis of the mechanism. The first of these, and possibly the one to be anticipated on the basis of the size and shape of the crystals, is the contracting sphere formula. The derivation supposes the eventual formation of an interface between reactant and product. This interface then moves from the surface inward in the form of a "contracting sphere." The expression, easily derived, is

$$(1 - \alpha)^{1/3} = Kt + c. \qquad (2)$$

This law has been used successfully in the decomposition of silver carbonate, magnesium hydroxide, and calcium carbonate hexahydrate.

Another equally attractive possibility is the following. In a polycrystalline sample there is no reason to believe that all the crystals will nucleate simultaneously. Thus, if one allows random nucleation of particles according to an exponential nucleation law followed by rapid surface growth of any particle nucleated, it is possible to arrive at the following expression for the rate of reaction of both parallelepipeds and spheres:

$$\ell n(1 - \alpha) = K_1 t + c, \tag{3}$$

where $\frac{dN}{dt} = K_1 N_o e^{-K_1 t}$, and K_1 = nucleation constant.

It is also possible to go one step further in sophistication by allowing for ingestion of nucleation sites and overlapping of nuclei. It is obvious that certain nuclei are no longer effective and that any expression for the amount of reacted material will give results that are too high. The expression derived does not allow solution, but if an assumption is made concerning the relationship of the actual percent reaction to the percent reaction which would appear if no ingestion and overlapping occurred, the following equations valid in the later stages of reaction may be derived:

$$\left[\ell n\,(1 - \alpha)^{1/3}\right] = Kt + c\,. \tag{4}$$

This expression is sometimes known as the Avrami-Erofeyev equation.

Finally, the case of random nucleation of crystals followed by the growth of compact linear nuclei is represented in the early stages of reaction by

$$\alpha = Kt^2 + c\,. \tag{5}$$

B. Calculation of Equilibrium-Vacancy Concentration in Rutile

Assume the following reaction:

$$2Ti^{+4} + O^{=} \rightarrow (AV) + 2Ti^{+3} + \frac{1}{2} O_2 ; \qquad (1)$$

then, $K_{eq} = n_{AV} \cdot n^2_{Ti^{+3}} \cdot P_{O_2}^{1/2} = \exp \frac{-\Delta F°}{RT} = \exp \frac{\Delta S}{R} \exp \frac{-\Delta H}{RT}$,

where K_{eq} = equilibrium constant for the reaction,
n_{AV} = mole fraction of anion vacancies,
$n_{Ti^{+3}}$ = mole fraction of Ti^{+3} ions,
P_{O_2} = oxygen pressure,
$\Delta F°$ = the change in Gibbs free energy for Eq. 1
$\Delta H°$ = the enthalpy change = $H_{AV} + 2H_{Ti^{+3}} + \frac{1}{2} H_{O_2}$

and

ΔS = the entropy change.

Experimentally,[50] we have $\Delta S°_{O_2} = 60$ cal/°C, $\Delta H° = 83{,}000 \pm 10$ kcal/mole.

Assume

$$n_{Ti^{+3}} = 2n_{AV}, \qquad \text{then} \qquad K_{eq} = 4n^3_{AV} \cdot P_{O_2}^{1/2} .$$

With P_{O_2} = 0.2 atm, the values of n_{AV} listed in Table VIII were calculated at T = 950°, 1000°, and 1050°C.

REFERENCES

1. F. C. Kracek, Melting and Transformation Temperatures of Minerals and Allied Substances, U. S. Geol. Surv. Bull. No. 1144D, U. S. Gov. Printing Office, Washington, 1963.
2. F. Barblan, E. Brandenberger, and P. Niggli, Geregelte und ungeregelte Strukturen von Titanaten und Ferriten und geregelte Umwandlungen der TiO_2 — Modifikationen, Helv. Chim. Acta 27, 88-96 (1958).
3. C. N. R. Rao, S. R. Yoganarasimhan and P. A. Faeth, Studies on the Brookite-Rutile Transformation, Trans. Faraday Soc. 57 (3), 504-510 (1961).
4. Y. Iida and S. Ozaki, "Grain Growth and Phase Transformation of Titanium Oxide During Calcination," J. Am. Ceram. Soc. 44 (3), 120-127 (1961).
5. C. N. R. Rao, A. Turner and J. M. Honig, Some Observations Concerning the Effect of Impurities on the Anatase-Rutile Transition, J. Phys. Chem. Solids 11 (1), 173-175 (1959).
6. A. W. Czanderna, C. N. R. Rao, and J. M. Honig, The Anatase-Rutile Transformation, Part I, Kinetics of the Transformation of Pure Anatase, Trans. Faraday Soc. 54 (7), 1069-1073 (1958).
7. W. F. Sullivan and S. Cole, Thermal Chemistry of Colloidal Titanium Dioxide, J. Am. Ceram. Soc. 42 (3) 127-133 (1959).
8. C. N. R. Rao, Kinetics and Thermodynamics of the Crystal Structure Transformation of Spectroscopically Pure Anatase to Rutile, Can. J. Chem. 39, 498-500 (1961).
9. F. K. Lotgering, Topotactical Reactions with Ferrimagnetic Oxides Having Hexagonal Crystal Structures, J. Inorg. Nucl. Chem. 9, 113-123 (1959).
10. R. D. Shannon and R. C. Rossi, The Definition of Topotaxy, Lawrence Radiation Laboratory Report UCRL-10957, Aug. 8, 1963 (to be published in Nature).

11. J. D. Bernal, On Topotaxy, Schweiz. Arch. angew. Wiss. Tech. 26, 69-75 (1960).

12. A. L. Mackay, Some Aspects of the Topochemistry of the Iron Oxides and Hydroxides, Proc. 4th Intern. Symp. Reactivity Solids, Reactivity of Solids, J. H. de Boer, ed., Amsterdam (1960), pp. 571-583.

13. L. S. Dent Glasser, F. D. Glasser, H. F. W. Taylor, Topotactic Reactions in Inorganic Oxycompounds, Quart. Rev. Chem. Soc. 16 (4), 343-360 (1962).

14. C. D. West, Orientation of Crystallites in the Ignition Products of $Mg(OH)_2$ and $Ca(OH)_2$, Am. Mineralogist 19 (6), 281-284 (1934).

15. A. C. D. Chaklader, X-ray Study of Quartz-Cristobalite Transformation, J. Am. Ceram. Soc. 46 (2), 66-71 (1963).

16. N. F. M. Henry, H. Lipson, and W. A. Wooster, The Interpretation of X-Ray Diffraction Photographs, 2nd ed. (Macmillan and Co., London, 1960), Chap. 9.

17. A. F. Wells, Structural Inorganic Chemistry (The Clarendon Press, Oxford, 1962), Chap. 23.

18. F. D. Glasser and L. S. Dent Glasser, Silicate Transformations: Rhodonite-Wollastonite, Acta Cryst. 14, 818-822 (1961).

19. W. D. Scott and J. A. Pask, Nucleation and Growth of Sodium Disilicate Crystals in Sodium Disilicate Glass, J. Am. Ceram. Soc. 44 (4), 181-187 (1961).

20. M. Bauer, Über die Paramorphosen von Rutil nach Anatas, N. Jb. Min. BB, 16, 392-394 (1903).

21. O. Mügge, Die regelmässigen Verwachsungen von Mineralen verschiedener Art, N. Jb. Min. Geol. Paleon. 1, 232-250 (1891).

22. W. E. Garner, The Kinetics of Endothermic Solid Reactions, in Chemistry of the Solid State, ed. by W. E. Garner, (Butterworth Scientific Publications, London, 1955) pp. 213-253.

23. H. P. Klug and L. E. Alexander, X-Ray Diffraction Procedures for Polycrystalline and Amorphous Materials, (John Wiley and Sons, Inc., New York, 1954).

24. H. E. Swanson and E. Tatge, Standard X-Ray Diffraction Powder Patterns, Nat. Bur. Std. (U. S.) Circ. No. 1, 539 (1953).

25. P. W. M. Jacobs and F. C. Tompkins, Classification and Theory of Solid Reactions in Chemistry of the Solid State, W. E. Garner, ed. (Academic Press, Inc., New York, 1955), pp. 184-212.

26. W. F. Sullivan and J. R. Coleman, Effect of Sulfur Trioxide on the Anatase-Rutile Transformation, J. Inorg. Nucl. Chem. 24, 645-661 (1962).

27. H. Knoll and U. Kühnhold, Über die Stabilität des Anatas, Naturwissenschaften 44 (14), 394 (1957).

28. O. W. Flörke, Über die Trübungsmittel Titandioxyd und Antimon - III - Oxyd, Mitt. Ver. Deut. Emailfachleute 6, 49-52 (1958).

29. I. J. Krchma and J. E. Booge, TiO_2 Manufacture, U. S. Pat. 2,462,978 (March 1, 1949); Ceram. Abstr., 1949, Sept., p. 219b.

30. H. H. Schaumann, "Production of TiO_2 Pigments," U. S. Pats. 2,488,439 (Nov. 15, 1949) and 2,488,440 (Nov. 14, 1949).

31. H. J. Cauwenberg and H. L. Sanders, "Methods of Producing Rutile," U. S. Pat. 2,477,559 (Aug. 2, 1949).

32. Carl Olson, "TiO_2 Pigment Production," U. S. Pat. 2,479,637 (Aug. 23, 1949).

33. G. Nodop, "Beitrag zur Kenntnis von Anatas, Rutil und Zinnstein" Hamburger Beitr. Angew. Mineral. Kristallphysik (Berlin) 1, 229-284 (1956).

34. R. E. Reeves and F. A. Blouin, Evidence of Polymerization in Titanium (IV) Sulfate Solutions, J. Am. Chem. Soc. 76, 5233-5235 (1954).

35. P. Kofstad, Thermogravimetric Studies of the Defect Structure of Rutile (TiO_2), J. Phys. Chem. Solids 23, 1579-1586 (1962).

36. P. Kofstad, K. Hauffe, and H. Kjöllesdal, Investigation on the Oxidation Mechanism of Titanium, Acta Chem. Scand. 12, 239-266 (1958).

37. R. D. Carnahan and J. O. Brittain, Point Defect Relaxation in Rutile Single Crystals, J. Appl. Phys. 34 (10), 3095-3104 (1963).

38. J. B. Wachtman, Jr. and L. R. Doyle, Internal Friction in Rutile Containing Point Defects, to be published by Phys. Rev.

39. J. Rudolph, Über den Leitungsmechanismus oxydischer Halbleiter bei hohen Temperaturen, Z. Naturforsch. 14a 727-737 (1959).

40. D. S. Tannhauser, Experimental Evidence from Conductivity Measurements for Interstitial Titanium in Reduced TiO_2, Solid State Communications 1, 223-225 (1963).

41. P. F. Chester, Electron Spin Resonance in Semiconducting Rutile, J. Appl. Phys. Supp. 32 (10), 2233-36 (1961).

42. J. Yahia, Dependence of the Electrical Conductivity and Thermoelectric Power of Pure and Aluminum-doped Rutile on Equilibrium Oxygen Pressure and Temperature, Phys. Rev. 130 (5), 1711-1719 (1963).

43. M. E. Straumanis, T. Ejima, and W. J. James, The TiO_2 Phase Explored by the Lattice Constant and Density Method, Acta Cryst. 14, 493-97 (1961).

44. S. Anderson, B. Collén, U. Kuylanstierna and A. Magnéli, Phase Analysis Studies on the Titanium-Oxygen System, Acta Chem. Scand. 11, 1641-1652 (1957).

45. R. N. Blumenthal and D. H. Whitmore, Thermodynamic Study of Phase Equilibria in the Titanium-Oxygen System within the $TiO_{1.95}$-TiO_2 Region, J. Electrochem Soc. 110 (1), 92-93 (1963).

46. N. W. Taylor, The Crystal Structure of the Compounds $ZnTiO_4$, $ZnTiO_4$, $ZnSnO_4$, Ni_2SiO_4, and $NiTiO_3$, Z. Physik Chem. 9B, 241-64 (1930).

47. S. K. Misra and A. C. D. Chaklader, The System Copper Oxide-Alumina, J. Am. Ceram. Soc. 46 (10), 509 (1963).

48. R. Lecuir and R. Lecuir, Electron Diffraction Study of Dehydration and Decomposition of Salts, Compt. Rend. 234, 93-95 (1952).

49. W. R. Buessem and S. R. Butler, Defect Reactions in TiO_2, in Kinetics of High Temperature Processes, ed. by W. D. Kingery (John Wiley and Sons, Inc., New York, 1959) pp. 13-19.

50. F. Seitz, On the Porosity Observed in the Kirkendall Effect, Acta Met. 1, 355-369 (1953).

This report was prepared as an account of Government sponsored work. Neither the United States, nor the Commission, nor any person acting on behalf of the Commission:

A. Makes any warranty or representation, expressed or implied, with respect to the accuracy, completeness, or usefulness of the information contained in this report, or that the use of any information, apparatus, method, or process disclosed in this report may not infringe privately owned rights; or

B. Assumes any liabilities with respect to the use of, or for damages resulting from the use of any information, apparatus, method, or process disclosed in this report.

As used in the above, "person acting on behalf of the Commission" includes any employee or contractor of the Commission, or employee of such contractor, to the extent that such employee or contractor of the Commission, or employee of such contractor prepares, disseminates, or provides access to, any information pursuant to his employment or contract with the Commission, or his employment with such contractor.